

High-dimensional Sobolev tests on hyperspheres

Bruno Ebner¹, Eduardo García-Portugués^{2,4}, and Thomas Verdebout³

Abstract

We derive the limit null distribution of the class of Sobolev tests of uniformity on the hypersphere when the dimension and the sample size diverge to infinity at arbitrary rates. The limiting non-null behavior of these tests is obtained for a sequence of integrated von Mises–Fisher local alternatives. The asymptotic results are applied to test for high-dimensional rotational symmetry and spherical symmetry. Numerical experiments illustrate the derived behavior of the uniformity and spherically symmetry tests under the null and under local and fixed alternatives.

Keywords: Directional statistics; Normality; Rotational symmetry; Spherical symmetry; Uniformity.

1 Introduction

Testing the uniformity of a sample of n independent and identically distributed random vectors $\mathbf{X}_1, \dots, \mathbf{X}_n$ on the unit (hyper)sphere $\mathbb{S}^d := \{\mathbf{x} \in \mathbb{R}^{d+1} : \mathbf{x}^\top \mathbf{x} = 1\}$, $d \geq 1$, is a classical testing problem that has generated a considerable number of contributions. A relatively reasonable number of available tests are described in García-Portugués and Verdebout (2018). One of the most overarching frameworks for testing uniformity on \mathbb{S}^d is the class of *Sobolev tests*, a term coined by Giné (1975) to reflect their relation with Sobolev norms. This class of tests has been introduced in Beran (1968) and Giné (1975), and contains the famous Rayleigh (1919) and Bingham (1974) tests, respectively based on the sample average and sample covariance matrix. Sobolev tests reject the null hypothesis of uniformity for large values of statistics of the form

$$S_n := \frac{1}{n} \sum_{i,j=1}^n \sum_{k=1}^{\infty} v_{k,d}^2 h_k(\mathbf{X}_i^\top \mathbf{X}_j), \quad h_k(x) := \begin{cases} 2 \cos(k \cos^{-1}(x)), & \text{if } d = 1, \\ (1 + \frac{2k}{d-1}) C_k^{(d-2)/2}(x), & \text{if } d > 1, \end{cases} \quad (1)$$

where $(v_{k,d})_{k=1}^{\infty}$ is a real sequence and $C_k^{(d-2)/2}$ is a Gegenbauer polynomial (see Section 2). Data-driven Sobolev tests have been proposed in Bogdan et al. (2002) for the circular case, and on compact Riemannian manifolds by Jupp (2008, 2009). The low-dimensional asymptotic behavior of Sobolev tests has been studied in Giné (1975), while detection thresholds under rotationally symmetric alternatives have been obtained recently in García-Portugués et al. (2024).

The interest raised by high-dimensional statistics in the last decade has also affected inference problems for directions. High-dimensional directional data has been considered in Dryden (2005), with applications in brain shape modeling, and in Banerjee et al. (2005), with applications to text mining, to name but a few. Within uniformity testing, Cuesta-Albertos et al. (2009) proposed a projection-based test that performs well empirically even in high dimensions, Paindaveine and Verdebout (2016) studied the high-dimensional null behavior of the Rayleigh test, while Cutting et al. (2017, 2022) focused on the high-dimensional asymptotic power of the Rayleigh and Bingham tests. Chikuse (1991, 1993) also explicitly considered high-dimensional testing for uniformity on the sphere in a fixed- n large- d framework, while Cai et al. (2013) rather adopted a double asymptotic approach for the same problem.

¹Institute of Stochastics, Karlsruhe Institute of Technology (Germany)

²Department of Statistics, Universidad Carlos III de Madrid (Spain).

³Department of Mathematics, Université libre de Bruxelles (Belgium).

⁴Corresponding author. e-mail: edgarcia@est-econ.uc3m.es.

The high-dimensional limiting behavior of (general) Sobolev tests remains largely unexplored. The present paper fills this gap by deriving the null asymptotic distributions of a general Sobolev statistic on \mathbb{S}^{d_n} as the dimension d_n diverges to infinity as the sample size n does. Additionally, the high-dimensional non-null behavior of Sobolev tests against integrated von Mises–Fisher alternatives is derived. We highlight that no assumptions on the rates of growth of n and d_n are imposed in these two results, and that they generalize the null and non-null high-dimensional findings by Paindaveine and Verdebout (2016) and Cutting et al. (2017) for the Rayleigh test. Applications of the high-dimensional limit results are then presented for testing rotational symmetry on the hypersphere \mathbb{S}^{d_n} and testing spherical symmetry on \mathbb{R}^{d_n+1} . Numerical experiments in the form of Monte Carlo simulations are shown to corroborate the asymptotic findings. The appendix contains the proofs and complementary numerical experiments.

The rest of this paper is organized as follows. Section 2 contains the main results on the null and non-null behavior of high-dimensional Sobolev tests of uniformity on \mathbb{S}^d . Applications to testing high-dimensional rotational symmetry on \mathbb{S}^d and spherical symmetry on \mathbb{R}^{d+1} are given in Section 3. Section 4 provides numerical experiments on testing high-dimensional spherical symmetry. A discussion is given in Section 5. Appendix A and B give the proofs of the presented results, while Appendix C shows an empirical illustration of the main asymptotic results.

2 Main results

2.1 General setup

Let $\mathbf{X}_{n,i}$, $i = 1, \dots, n$, $n = 1, 2, \dots$, be a triangular array of random vectors where, for any n , the $\mathbf{X}_{n,i}$'s are mutually independent and share a common distribution on the unit sphere $\mathbb{S}^{d_n} = \{\mathbf{x} \in \mathbb{R}^{d_n+1} : \mathbf{x}^\top \mathbf{x} = 1\}$. We consider the problem of testing the null hypothesis $\mathcal{H}_{0,n}$ stating that this common distribution is the uniform over \mathbb{S}^{d_n} when n and d_n diverge to infinity.

The Sobolev statistics (1) are based on the Gegenbauer polynomials $\{C_k^{(d-1)/2}\}_{k=1}^\infty$ of index $(d-1)/2$, $d \geq 2$, which form an orthogonal basis on the space of square-integrable real functions in $[-1, 1]$ with respect to the weight $x \mapsto (1-x^2)^{d/2-1}$. More precisely, they satisfy

$$\int_{-1}^1 C_k^{(d-1)/2}(x) C_\ell^{(d-1)/2}(x) (1-x^2)^{d/2-1} dx = \delta_{k,\ell} c_{k,d}, \quad (2)$$

where $\delta_{k,\ell}$ represents the Kronecker delta and

$$c_{k,d} := \frac{2^{3-d} \pi \Gamma(d+k-1)}{(d+2k-1)k! \Gamma((d-1)/2)^2} = \frac{\omega_d}{\omega_{d-1}} \left(1 + \frac{2k}{d-1}\right)^{-2} d_{k,d}, \quad (3)$$

with $\omega_d := 2\pi^{(d+1)/2} / \Gamma((d+1)/2)$ denoting the surface area of \mathbb{S}^d . Above,

$$d_{k,d} := \binom{d+k-2}{d-1} + \binom{d+k-1}{d-1} = \left(1 + \frac{2k}{d-1}\right) \frac{\Gamma(d-1+k)}{\Gamma(d-1)k!} \quad (4)$$

is the dimension of the vector space that contains the collection of spherical harmonics of degree k . For more details see for instance Section 3 in García-Portugués et al. (2024).

2.2 Null behavior

In our first main result we study the high-dimensional asymptotic behavior under $\mathcal{H}_{0,n}$ of the general Sobolev test statistic

$$T_n := \frac{2}{n} \sum_{1 \leq i < j \leq n} \psi_n(\mathbf{X}_{n,i}^\top \mathbf{X}_{n,j})$$

with $\psi_n : [0, 1] \rightarrow \mathbb{R}$ defined almost everywhere as

$$\psi_n(x) := \sum_{k=1}^{\infty} \left(1 + \frac{2k}{d_n - 1}\right) v_{k,d_n}^2 C_k^{(d_n-1)/2}(x), \quad (5)$$

for a real sequence of weights $(v_{k,d_n})_{k=1}^{\infty}$ and $d_n \geq 2$. For $d_n = 1$, let

$$\psi_n(x) := \sum_{k=1}^{\infty} 2v_{k,1}^2 \cos(k \cos^{-1}(x))$$

(the terms of the series are generated by Chebyshev polynomials).

Theorem 2.1. *Let d_n be a sequence of positive integers such that $d_n \rightarrow \infty$ as $n \rightarrow \infty$. Assume that $\mathbf{X}_{n,i}$, $i = 1, \dots, n$, $n = 1, 2, \dots$ form a triangular array such that, for any fixed n , $\mathbf{X}_{n,1}, \dots, \mathbf{X}_{n,n}$ are mutually independent and uniformly distributed on \mathbb{S}^{d_n} . Assume moreover that:*

(i) *For every $n \geq 1$ and $d_n \geq 1$,*

$$\sigma_n^2 := 2\mathbb{E}[\psi_n^2(\mathbf{X}_{n,1}^\top \mathbf{X}_{n,2})] = 2 \sum_{k=1}^{\infty} v_{k,d_n}^4 d_{k,d_n} < \infty. \quad (6)$$

(ii) *As $n \rightarrow \infty$ and $d_n \rightarrow \infty$,*

$$\sigma_n^{-4} \sum_{k=1}^{\infty} v_{k,d_n}^8 d_{k,d_n} = o(1) \quad \text{and} \quad \sigma_n^{-4} \mathbb{E}[\psi_n^4(\mathbf{X}_{n,1}^\top \mathbf{X}_{n,2})] = O(1). \quad (7)$$

Then $\sigma_n^{-1} T_n \rightsquigarrow \mathcal{N}(0, 1)$, with \rightsquigarrow denoting weak convergence.

Remark 2.1. *As shown in the proof of Theorem 2.1, condition (7) is implied by*

$$\sigma_n^{-4} \mathbb{E}[\psi_n^4(\mathbf{X}_{n,1}^\top \mathbf{X}_{n,2})] = o(1). \quad (8)$$

For a fixed integer $k_0 \geq 1$, consider the sequence $v_{k,d_n} = \delta_{k,k_0}$, for $k \geq 1$, defining a “ k_0 -Sobolev test”. Then,

$$\psi_n(x) = \psi_{n,k_0}(x) := \left(1 + \frac{2k_0}{d_n - 1}\right) C_{k_0}^{(d_n-1)/2}(x)$$

and, because of Lemma B.1, $\mathbb{E}[\psi_{n,k_0}^4(\mathbf{X}_{n,1}^\top \mathbf{X}_{n,2})] \asymp d_n^{2k_0}$ (\asymp stands for exact order equality). Therefore, conditions (i) and (ii) hold, since $\sigma_n^2 = 2d_{k_0,d_n} \asymp d_n^{k_0} < \infty$ for every $n \geq 1$ and $d_n \geq 1$, and

$$\sigma_n^{-4} \sum_{k=1}^{\infty} \delta_{k,k_0} d_{k,d_n} \asymp d_n^{-2k_0} d_n^{k_0} = o(1) \quad \text{and} \quad \sigma_n^{-4} \mathbb{E}[\psi_n^4(\mathbf{X}_{n,1}^\top \mathbf{X}_{n,2})] \asymp d_n^{-2k_0} d_n^{2k_0} = O(1).$$

Since $d_{k_0,d_n} \sim (1 + 2k_0/(d_n - 1)) d_n^{k_0}/k_0!$ by Lemma B.1 (\sim for equality in the limit), Theorem 2.1 gives

$$\frac{\sqrt{2k_0!}}{d_n^{k_0/2} n} \sum_{1 \leq i < j \leq n} C_{k_0}^{(d_n-1)/2}(\mathbf{X}_{n,i}^\top \mathbf{X}_{n,j}) \rightsquigarrow \mathcal{N}(0, 1) \quad (9)$$

as $n \rightarrow \infty$ and $d_n \rightarrow \infty$. For $k_0 = 1$, the high-dimensional result in Paindaveine and Verdebout (2016, Theorem 2.1) for the Rayleigh statistic arises as a particular case in (9):

$$\frac{\sqrt{2d_n}}{n} \sum_{1 \leq i < j \leq n} \mathbf{X}_{n,i}^\top \mathbf{X}_{n,j} \sim \frac{\sqrt{2}}{d_n^{1/2} n} \sum_{1 \leq i < j \leq n} C_1^{(d_n-1)/2}(\mathbf{X}_{n,i}^\top \mathbf{X}_{n,j}) \rightsquigarrow \mathcal{N}(0, 1).$$

2.3 Non-null behavior

We explore now the situation where, for any n , $\mathbf{X}_{n,1}, \dots, \mathbf{X}_{n,n}$ share an *integrated von Mises–Fisher distribution* on \mathbb{S}^{d_n} with location parameter $\boldsymbol{\theta} \in \mathbb{S}^{d_n}$ and varying concentration parameter $\kappa_n \geq 0$ (with $\kappa_n = 0$ corresponding to uniformity). Such alternatives are characterized by likelihood functions (with respect to the surface area measure on \mathbb{S}^{d_n}) of the form

$$\frac{d\mathbf{P}_{\kappa_n}^{(n)}}{dm_{d_n}} = c_{d_n, \kappa_n} \int_{\text{SO}(d_n+1)} \prod_{i=1}^n \exp(\kappa_n \mathbf{X}_{n,i}^\top \mathbf{O}\boldsymbol{\theta}) d\mathbf{O}, \quad (10)$$

where c_{d_n, κ_n} is a normalising constant and the integral is with respect to the Haar measure on $\text{SO}(d_n+1)$. Unlike the von Mises–Fisher distribution with density $\mathbf{x} \mapsto c_{d_n, \kappa_n} \exp(\kappa_n \mathbf{x}^\top \boldsymbol{\theta})$, the integrated von Mises–Fisher distribution is invariant with respect to rotations. This invariance justifies its choice for analysing the power of uniformity tests, as these are obviously invariant with respect to rotations and thus their asymptotic power cannot depend on $\boldsymbol{\theta}$. As shown in Cutting et al. (2017, Theorem 4.2), the Rayleigh test enjoys asymptotic non-trivial powers against such integrated von Mises–Fisher alternatives with $\kappa_n \asymp d_n^{3/4}/\sqrt{n}$.

The following result gives the high-dimensional asymptotic power of Sobolev tests against alternatives where (10) holds, extending that in Cutting et al. (2017, Section 4.2) for the Rayleigh test.

Theorem 2.2. *Assume that the setup of Theorem 2.1 and its assumptions (i) and (ii) hold for the situation in which $\mathbf{X}_{n,1}, \dots, \mathbf{X}_{n,n}$ are distributed as integrated von Mises–Fisher on \mathbb{S}^{d_n} with concentration $\kappa_n = \tau_n d_n^{3/4}/\sqrt{n}$ for the positive sequence $\tau_n \rightarrow \tau > 0$.*

Then $\sigma_n^{-1}T_n \rightsquigarrow \mathcal{N}(\Gamma\tau^2, 1)$, where

$$\Gamma := \lim_{n \rightarrow \infty} \frac{\sqrt{d_n} v_{1, d_n}^2}{\sqrt{2} (\sum_{k=1}^{\infty} v_{k, d_n}^4 d_{k, d_n})^{1/2}}. \quad (11)$$

As a consequence of Theorem 2.2, the test that rejects at the asymptotic level α when $\sigma_n^{-1}T_n > z_\alpha$, where z_α is the α -upper quantile of a standard normal, has asymptotic power $1 - \Phi(z_\alpha - \Gamma\tau^2)$ against contiguous alternatives given by integrated von Mises–Fisher distributions with $\kappa_n = \tau_n d_n^{3/4}/\sqrt{n}$. Therefore, it is able to detect such alternatives if and only if $\Gamma > 0$. Since $d_{k_0, d_n} \sim d_n^{k_0}/k_0!$, we have two relevant implications:

- For the subclass of k_0 -Sobolev tests with $v_{k, d_n} = \delta_{k, k_0}$, $\Gamma = (1/\sqrt{2})1_{\{k_0=1\}}$. Therefore, the Rayleigh test is the only of these tests detecting the studied contiguous alternatives. In particular, the Bingham test with $v_{k, d_n} = \delta_{k, 2}$ is “blind” against them.
- For the subclass of *finite Sobolev tests* with $v_{k, d_n} = 1_{\{k \leq k_0\}}$, for $k_0 > 1$, $\Gamma = 0$. Therefore, none of these tests can detect the studied contiguous alternatives, despite the similarity between the Rayleigh sequence $v_{k, d_n} = \delta_{k, 1}$ and, e.g., the “hybrid Rayleigh–Bingham” test arising with $v_{k, d_n} = \delta_{k, 1} + \delta_{k, 2}$.

It is possible to combine the Rayleigh test with other Sobolev tests in a way that the resulting test is still able to detect contiguous integrated von Mises–Fisher alternatives. This can be achieved by making the sequence of weights $(v_{k, d_n})_{k=1}^{\infty}$ to decay with d_n . Indeed, it is immediate to check that the weights $(v_{k, d_n})_{k=1}^{\infty}$ that, given $v_{1, d_n} = 1$, result in $0 < \Gamma \leq 1/\sqrt{2}$ are characterized as $v_{k, d_n} \asymp [c_{k, d_n} k! d_n^{-(k-1)}]^{1/4}$ for $k > 1$ and sequence $(c_{k, d_n})_{k=1}^{\infty}$ such that $\sum_{k=2}^{\infty} c_{k, d_n} = O(1)$, with $\Gamma = 1/\sqrt{2}$ attained with $(c_{k, d_n})_{k=1}^{\infty}$ such that $\sum_{k=2}^{\infty} c_{k, d_n} = o(1)$.

Appendix C reports numerical experiments illustrating Theorems 2.1–2.2 and the effect of the above-discussed sequences of weights on the local power.

3 Testing applications

3.1 Rotational symmetry

A random vector \mathbf{X} on \mathbb{S}^{d_n} has a *rotationally symmetric* distribution about $\boldsymbol{\theta} \in \mathbb{S}^{d_n}$ if and only if $\mathbf{O}\mathbf{X}$ has the same distribution as \mathbf{X} for any orthogonal matrix $\mathbf{O} \in \text{SO}(d_n + 1)$ such that $\mathbf{O}\boldsymbol{\theta} = \boldsymbol{\theta}$. Rotational symmetry is closely related with the *tangent-normal decomposition*: for any $\mathbf{x} \in \mathbb{S}^{d_n}$,

$$\mathbf{x} = v_{\boldsymbol{\theta}}(\mathbf{x})\boldsymbol{\theta} + (1 - v_{\boldsymbol{\theta}}^2(\mathbf{x}))^{1/2} \boldsymbol{\Gamma}_{\boldsymbol{\theta}} \mathbf{u}_{\boldsymbol{\theta}}(\mathbf{x}), \quad v_{\boldsymbol{\theta}}(\mathbf{x}) := \mathbf{x}^\top \boldsymbol{\theta}, \quad \mathbf{u}_{\boldsymbol{\theta}}(\mathbf{x}) := \frac{\boldsymbol{\Gamma}_{\boldsymbol{\theta}}^\top \mathbf{x}}{\|\boldsymbol{\Gamma}_{\boldsymbol{\theta}}^\top \mathbf{x}\|}, \quad (12)$$

where $\boldsymbol{\Gamma}_{\boldsymbol{\theta}}$ denotes an arbitrary $(d_n + 1) \times d_n$ matrix whose columns form an orthogonal complement to $\boldsymbol{\theta}$ (so that $\boldsymbol{\Gamma}_{\boldsymbol{\theta}}^\top \boldsymbol{\Gamma}_{\boldsymbol{\theta}} = \mathbf{I}_{d_n}$ and $\boldsymbol{\Gamma}_{\boldsymbol{\theta}} \boldsymbol{\Gamma}_{\boldsymbol{\theta}}^\top = \mathbf{I}_{d_n+1} - \boldsymbol{\theta}\boldsymbol{\theta}^\top$). If \mathbf{X} is rotationally symmetric about $\boldsymbol{\theta}$, then the *multivariate sign* $\mathbf{u}_{\boldsymbol{\theta}}(\mathbf{X})$ is uniformly distributed over \mathbb{S}^{d_n-1} . Therefore, based on a sample $\mathbf{X}_{n,1}, \dots, \mathbf{X}_{n,n}$ on \mathbb{S}^{d_n} , one way to test for rotational symmetry about $\boldsymbol{\theta}$ is to test the necessary condition of the uniformity of $\mathbf{u}_{\boldsymbol{\theta}}(\mathbf{X}_{n,1}), \dots, \mathbf{u}_{\boldsymbol{\theta}}(\mathbf{X}_{n,n})$ on \mathbb{S}^{d_n-1} .

The tangent von Mises–Fisher distribution defined in García-Portugués et al. (2020, Section 2.2) provides a set of alternatives to rotational symmetry about $\boldsymbol{\theta}$ based on (12). A random vector \mathbf{X} on \mathbb{S}^{d_n} has such distribution if $v_{\boldsymbol{\theta}}(\mathbf{X})$ follows an arbitrary density g on $[-1, 1]$, $\mathbf{u}_{\boldsymbol{\theta}}(\mathbf{X})$ is von Mises–Fisher distributed with location $\boldsymbol{\mu} \in \mathbb{S}^{d_n-1}$ and concentration $\kappa_n \geq 0$ (with $\kappa_n = 0$ corresponding to rotational symmetry about $\boldsymbol{\theta}$), and $v_{\boldsymbol{\theta}}(\mathbf{X})$ and $\mathbf{u}_{\boldsymbol{\theta}}(\mathbf{X})$ are independent. As in (10), an *integrated tangent von Mises–Fisher distribution* is characterized by the likelihood function

$$\frac{dP_{\boldsymbol{\theta}, g, \kappa_n}^{(n)}}{dm_{d_n}} = c_{d_n, g, \kappa_n} \prod_{i=1}^n g(v_{\boldsymbol{\theta}}(\mathbf{X}_{n,i})) \int_{\text{SO}(d_n)} \prod_{i=1}^n \exp(\kappa_n \mathbf{u}_{\boldsymbol{\theta}}(\mathbf{X}_{n,i})^\top \mathbf{O}\boldsymbol{\mu}) d\mathbf{O}. \quad (13)$$

We have the following result as a direct consequence of Theorem 2.2, (10), and (13).

Corollary 3.1. *Let d_n be a sequence of positive integers such that $d_n \rightarrow \infty$ as $n \rightarrow \infty$. Assume that $\mathbf{X}_{n,i}$, $i = 1, \dots, n$, $n = 1, 2, \dots$ form a triangular array such that, for any fixed n , the random vectors $\mathbf{X}_{n,1}, \dots, \mathbf{X}_{n,n}$ are mutually independent and distributed as integrated tangent von Mises–Fisher about $\boldsymbol{\theta} \in \mathbb{S}^{d_n}$ with concentration $\kappa_n = \tau_n d_n^{3/4} / \sqrt{n}$ for the positive sequence $\tau_n \rightarrow \tau > 0$. Assume moreover that assumptions (i) and (ii) of Theorem 2.1 hold for the sample $\mathbf{u}_{\boldsymbol{\theta}}(\mathbf{X}_{n,1}), \dots, \mathbf{u}_{\boldsymbol{\theta}}(\mathbf{X}_{n,n})$, and that T_n is computed on this sample.*

Then $\sigma_n^{-1} T_n \rightsquigarrow \mathcal{N}(\Gamma\tau^2, 1)$ with Γ given in (11).

3.2 Spherical symmetry

A random vector \mathbf{X} on \mathbb{R}^{d_n+1} has a *spherically symmetric* distribution if and only if $\mathbf{O}\mathbf{X}$ has the same distribution as \mathbf{X} for any orthogonal matrix $\mathbf{O} \in \text{SO}(d_n + 2)$. In the absolutely continuous case, spherical symmetry of \mathbf{X} is characterized by the projection $\pi(\mathbf{X}) := \mathbf{X}/\|\mathbf{X}\|$ being uniformly distributed over \mathbb{S}^{d_n} and the radius $\|\mathbf{X}\|$ being independent from $\pi(\mathbf{X})$. Therefore, based on a sample $\mathbf{X}_{n,1}, \dots, \mathbf{X}_{n,n}$ on \mathbb{R}^{d_n+1} , one way to test for spherical symmetry is to test the necessary condition of the uniformity of $\pi(\mathbf{X}_{n,1}), \dots, \pi(\mathbf{X}_{n,n})$ on \mathbb{S}^{d_n} , where Theorem 2.1 is applicable.

The previous characterisation of spherical symmetry can be exploited to construct high-dimensional goodness-of-fit tests for distributions on \mathbb{R}^{d_n+1} , i.e., test

$$\mathcal{H}_{0,n} : \mathbf{X}_{n,1}, \dots, \mathbf{X}_{n,n} \text{ share the distribution } F_{0,n} \quad (14)$$

for a specified distribution $F_{0,n}$ on \mathbb{R}^{d_n+1} . For that purpose, we only need a classical (one-dimensional) goodness-of-fit test for the common radial distribution $R_{0,n}$ of the sample $\|\mathbf{X}_{n,1}\|, \dots, \|\mathbf{X}_{n,n}\|$ that is induced by $F_{0,n}$. Let A_n denote a test statistic for this purpose, such as the Anderson–Darling test statistic, and let $F_A(x) := \lim_{n \rightarrow \infty} \Pr[A_n \leq x]$, $x \geq 0$, be the null asymptotic distribution

of A_n . Then, given the sample $\mathbf{X}_{n,1}, \dots, \mathbf{X}_{n,n}$ on \mathbb{R}^{d_n+1} , we can test (14) by testing: (i) that $\|\mathbf{X}_{n,1}\|, \dots, \|\mathbf{X}_{n,n}\|$ share the radial distribution $R_{0,n}$; (ii) that $\pi(\mathbf{X}_{n,1}), \dots, \pi(\mathbf{X}_{n,n})$ are uniformly distributed on \mathbb{S}^{d_n} ; and (iii) that the previous samples are independent. We can do (i–iii) through the statistic resulting from the Fisher aggregation of p -values (Fisher, 1925)

$$G_n := -2[\log(1 - F_A(A_n)) + \log(1 - \Phi(T_n))],$$

where A_n is computed with $\|\mathbf{X}_{n,1}\|, \dots, \|\mathbf{X}_{n,n}\|$ and T_n is computed with $\pi(\mathbf{X}_{n,1}), \dots, \pi(\mathbf{X}_{n,n})$. Under the null hypothesis in (14), as $d_n \rightarrow \infty$ with $n \rightarrow \infty$, the asymptotic distribution of G_n is χ_2^2 . Some particularly relevant cases for the distribution F_{0,d_n} in (14) are:

- Multivariate standard normal $\mathcal{N}_{d_n+1}(\mathbf{0}, \mathbf{I}_{d_n+1})$, where $\|\mathbf{X}\|^2$ follows a $\chi_{d_n+1}^2$ distribution.
- Multivariate standard Student's t distribution with $\nu > 0$ degrees of freedom, where $\|\mathbf{X}\|^2/(d_n+1)$ follows Snedecor's $F_{d_n+1,\nu}$ distribution.
- Multivariate isotropic stable distribution, where $\|\mathbf{X}\|^2$ is distributed as the product AT , where A follows a positive stable law $S(\beta/2, 1, 2\gamma_0^2(\cos(\pi\beta/4))^{2/\beta}, 0)$, $0 < \beta < 2$, $\gamma_0 > 0$, and T independently follows a $\chi_{d_n+1}^2$ distribution (Nolan, 2013).

The simple null hypothesis tested in (14) can be generalized to the composite null

$$\mathcal{H}_{0,n} : \mathbf{X}_{n,1}, \dots, \mathbf{X}_{n,n} \text{ share the distribution } F_{0,n,\boldsymbol{\theta}} \quad (15)$$

with $\boldsymbol{\theta} \in \Theta \subset \mathbb{R}^q$ an unknown parameter only affecting the radial distribution $R_{0,n,\boldsymbol{\theta}}$ of $\|\mathbf{X}_{n,1}\|, \dots, \|\mathbf{X}_{n,n}\|$. In this case, the above testing pipeline has to be only modified in the radial part to carry out a parametric goodness-of-fit test, with A_n suitably adapted and F_A potentially approximated by parametric bootstrapping. A relevant case of (15) is the high-dimensional goodness-of-fit for spherically symmetric distribution on \mathbb{R}^{d_n+1} with squared radius distributed as $\Gamma(\theta_1, \theta_2)$, which in particular comprises standard normality for $\theta_1 = (d_n+1)/2$ and $\theta_2 = 2$. Another interesting case is the multivariate t distribution where the degrees of freedom ν are unknown and have to be estimated.

4 Numerical experiments

We present the results of a quadripartite Monte Carlo simulation study conducted to demonstrate the power performance of the goodness-of-fit test for spherical symmetry presented in Section 3.2 in high-dimensional settings. For all four parts we used the following simulation setting. To test the radial component, we utilize the classical Anderson–Darling test in (14) and incorporating parameter estimation in (15). In the latter (composite) case we employ a bootstrap algorithm which is implemented as follows:

- Compute the estimator $\hat{\boldsymbol{\theta}}$ from the radial part of the data.
- Compute the Anderson–Darling test statistic A_n assuming $\hat{\boldsymbol{\theta}}$ is the underlying parameter.
- Generate B bootstrap samples from $R_{0,n,\hat{\boldsymbol{\theta}}}$, the estimated radial distribution (recall (15)).
- Compute for each bootstrap sample j the estimator $\tilde{\boldsymbol{\theta}}_j$ and compute $\tilde{A}_{n,j}$ assuming $\tilde{\boldsymbol{\theta}}_j$ is the underlying parameter, $j = 1, \dots, B$.
- Generate the bootstrap p -value $p_{A_n} = \frac{1}{B} \sum_{j=1}^B 1_{\{\tilde{A}_{n,j} > A_n\}}$.

In the final computation of G_n , the directional part of the data is kept fixed, and the bootstrap p -value p_{A_n} replaces the p -value of the radial part.

We conducted $M = 5,000$ Monte Carlo repetitions with a fixed significance level of 5%. When employing a bootstrap algorithm, we used $B = 500$ bootstrap samples. To construct alternatives to (14) and (15), we used the next models: $t_\nu(\mathbf{S})$, the centered multivariate t distribution with $\nu > 0$ degrees of freedom and scale matrix \mathbf{S} ; $st_\nu(\mathbf{S}, \boldsymbol{\xi})$, the skewed version of $t_\nu(\mathbf{S})$ by the skewing vector $\boldsymbol{\xi}$ (Azzalini, 2014); $\text{vMF}(\kappa)$, the von Mises–Fisher distribution with mean direction $(1, 0, \dots, 0)^\top$ and concentration $\kappa > 0$; $F \otimes G$ the law of $\mathbf{X} \cdot Y$, where \mathbf{X} is a random vector with distribution F and Y is a positive random variable with distribution G . We set $\boldsymbol{\xi}_1 = (1, 0, \dots, 0)^\top$ and $\boldsymbol{\Omega}_1$ as a matrix with ones on the diagonal and 0.25 in every off-diagonal entry. For the multivariate normal distribution, the covariance matrix is denoted by $\boldsymbol{\Sigma}_\rho = \text{diag}(0.5, \overset{[pd]}{\cdot}, 0.5, 1.5, \overset{d-[pd]}{\cdot}, 1.5)$. The identity matrix of size $d \times d$ is denoted as \mathbf{I}_d . The model DMN(ρ) (dependent multivariate normal), with $\rho \in [0, 1]$, is defined by $\mathbf{X} \cdot R$, where: $R = [F_d^{-1}(\Phi(Z))]^{1/2}$, with Φ and F_d being the distribution functions of a standard normal and a χ_d^2 , respectively; $\mathbf{X} = \mathbf{Y}/\|\mathbf{Y}\|$; and $(Z, \mathbf{Y}^\top)^\top$ is distributed as $\mathcal{N}_{d+1}(\mathbf{0}, \boldsymbol{\Sigma}_\rho)$ for $\boldsymbol{\Sigma}_\rho = (1, \boldsymbol{\rho}^\top; \boldsymbol{\rho}, \mathbf{I}_d)$ and $\boldsymbol{\rho} = (\rho^1, \dots, \rho^d)^\top$. Note that R and \mathbf{X} have the marginal distributions of the radial and projected components of $\mathcal{N}_d(\mathbf{0}, \mathbf{I}_d)$, but that dependence between R and \mathbf{X} is present if $\rho > 0$. We denote by $|F|$ the distribution of $|X|$ when X is distributed as F , $\text{Ca}(\mu, \gamma)$ refers to the Cauchy distribution with location parameter $\mu \in \mathbb{R}$ and scale parameter $\gamma > 0$, and $\Gamma(k, \theta)$ stands for a gamma distribution with shape $k > 0$ and scale $\theta > 0$. Lastly, $S(\beta) = S(\beta/2, 1, 2\gamma_0^2(\cos(\pi\beta/4))^{2/\beta}, 0)$, for $0 < \beta < 2$ and $\gamma_0 = 1$, denotes a positive stable law.

n	100						200							
	d	100	200	300	100	200	300	100	200	300	100	200	300	
Test		G_n			BHEP				G_n			BHEP		
$\mathcal{N}_d(\mathbf{0}, \mathbf{I}_d)$		5	5	5	5	1	0	5	5	5	5	1	0	
$\mathcal{N}_d(\mathbf{0}, \boldsymbol{\Sigma}_{0.1})$		5	6	6	7	2	1	6	6	5	9	2	1	
$\mathcal{N}_d(\mathbf{0}, \boldsymbol{\Sigma}_{0.25})$		8	8	7	12	3	1	8	9	9	20	6	1	
$\mathcal{N}_d(\mathbf{0}, \boldsymbol{\Sigma}_{0.5})$		14	13	14	22	6	2	19	20	20	48	14	5	
$\text{vMF}(1) \otimes [\chi_d^2]^{1/2}$		5	5	5	6	2	0	5	5	4	6	2	0	
$\text{vMF}(4) \otimes [\chi_d^2]^{1/2}$		18	7	5	29	3	1	49	12	7	65	8	1	
$t_{10}(0.75 \cdot \mathbf{I}_d)$		100	100	100	49	48	48	100	100	100	86	87	89	
$t_{10}(0.8 \cdot \mathbf{I}_d)$		100	100	100	14	12	10	100	100	100	32	31	30	
$t_{10}(0.9 \cdot \mathbf{I}_d)$		100	100	100	20	18	17	100	100	100	27	26	26	
$t_{10}(1.1 \cdot \mathbf{I}_d)$		100	100	100	100	100	100	100	100	100	100	100	100	
$t_{10}(\mathbf{I}_d)$		100	100	100	84	84	88	100	100	100	98	99	99	
$t_{30}(\mathbf{I}_d)$		100	100	100	21	18	15	100	100	100	32	31	30	
$t_{100}(\mathbf{I}_d)$		86	100	100	6	2	1	100	100	100	7	3	1	
$t_{500}(\mathbf{I}_d)$		9	21	43	6	1	0	13	40	76	5	1	0	
$t_{1000}(\mathbf{I}_d)$		6	9	14	5	1	0	7	13	23	5	1	0	

Table 1: Empirical rejection rates (in percentage) for testing high-dimensional normality in comparison to the simple hypothesis version of the BHEP test of multivariate normality.

In the first part of the simulation study, we provide results designed to demonstrate the power performance of the goodness-of-fit test of high-dimensional normality. As a benchmark, we selected the simple hypothesis version of the classical BHEP test for multivariate normality, which is based on the weighted L^2 distance between the characteristic function of the standard normal distribution and its empirical counterpart, as described in Ebner and Henze (2020). This test is equivalent to the one used in Henze and Wagner (1997), except that it applies the original data instead of scaled residuals. Critical values for the BHEP test, depending on the sample size n and dimension d , were obtained via Monte Carlo simulation with 100,000 repetitions. The results are presented in Table 1. We observe that both tests are well-calibrated, although the BHEP test appears conservative when $d > n$. In lower dimensions (e.g., $d = 100$), the BHEP test outperforms the new test for most

alternatives, except for the multivariate Student's t distribution. However, as the dimensionality increases ($d = 200, 300$), the new test significantly surpasses the BHEP test. Notably, for the t distribution, as the degrees of freedom increase and approach the null hypothesis, the new test retains power, while the BHEP test completely fails.

The second part of the simulation study is two-fold. First, we test the simple null hypothesis $\mathcal{H}_{0,n}$ as defined in (14), which posits that the data follows a multivariate standard Student distribution with a fixed degrees of freedom parameter ν . Second, we examine the composite hypothesis in (15), wherein the parameter ν is estimated using the maximum likelihood estimator with respect to the radial component of the data. In the finite-dimensional case, Meintanis et al. (2024) investigated the goodness-of-fit testing of the family of multivariate t distributions. Notably, all known methods provided or cited therein exhibit severe computational limitations as the dimension d increases, in some cases as early as $d \geq 5$. Therefore, to the best of our knowledge, the methodology presented herein is unrivaled.

n	100			200			500			1000			
	d	100	200	300	100	200	300	100	200	300	100	200	300
$t_5(\mathbf{I}_d)$	5	5	5	5	5	5	6	5	5	5	5	5	5
$t_6(\mathbf{I}_d)$	6	6	6	8	9	9	22	22	24	54	54	56	
$t_7(\mathbf{I}_d)$	13	12	13	28	29	30	82	85	85	100	100	100	
$t_8(\mathbf{I}_d)$	23	25	25	60	64	65	100	100	100	100	100	100	
$t_5(0.9 \cdot \mathbf{I}_d)$	26	26	26	47	48	49	86	88	88	99	100	100	
$\text{vMF}(5) \otimes [d \cdot \mathbf{F}_{d,5}]^{1/2}$	33	9	5	79	20	8	100	74	32	100	100	83	
$\text{vMF}(10) \otimes [d \cdot \mathbf{F}_{d,5}]^{1/2}$	100	55	21	100	97	61	100	100	100	100	100	100	
$st_5(\boldsymbol{\Omega}_1, \mathbf{0})$	28	40	48	37	49	59	63	72	78	87	92	95	
$st_5(\mathbf{I}_d, \boldsymbol{\xi}_1)$	48	28	20	96	76	61	100	100	100	100	100	100	
$st_8(\boldsymbol{\Omega}_1, \mathbf{0})$	44	55	62	69	77	81	97	99	99	100	100	100	
$st_8(\mathbf{I}_d, \boldsymbol{\xi}_1)$	71	55	47	100	97	94	100	100	100	100	100	100	
$t_5(\mathbf{I}_d)$	5	5	5	5	5	5	5	5	5	5	5	5	
$t_5(0.8 \cdot \mathbf{I}_d)$	85	87	87	99	99	99	100	100	100	100	100	100	
$t_5(0.9 \cdot \mathbf{I}_d)$	29	29	29	51	53	52	88	89	90	99	100	100	
$t_5(1.1 \cdot \mathbf{I}_d)$	20	19	21	36	39	38	78	79	81	98	99	99	
$t_5(1.25 \cdot \mathbf{I}_d)$	79	81	81	99	99	99	100	100	100	100	100	100	
$\text{vMF}(1) \otimes [d \cdot \mathbf{F}_{d,5}]^{1/2}$	4	5	4	6	4	4	6	5	6	12	5	6	
$\text{vMF}(3) \otimes [d \cdot \mathbf{F}_{d,5}]^{1/2}$	10	5	6	23	6	5	75	17	9	100	51	19	
$\text{vMF}(5) \otimes [d \cdot \mathbf{F}_{d,5}]^{1/2}$	33	9	5	80	20	11	100	76	29	100	100	80	
$\text{vMF}(10) \otimes [d \cdot \mathbf{F}_{d,5}]^{1/2}$	100	57	23	100	98	65	100	100	100	100	100	100	
$st_5(\boldsymbol{\Omega}_1, \mathbf{0})$	30	40	48	39	49	59	60	69	76	86	90	92	
$st_5(\mathbf{I}_d, \boldsymbol{\xi}_1)$	48	28	20	95	77	60	100	100	100	100	100	100	

Table 2: Empirical rejection rates (in percentage) for testing the fit to the high-dimensional multivariate Student distribution with known $\nu = 5$ degrees of freedom (top) and unknown degrees of freedom parameter estimated by maximum-likelihood (bottom).

The results in Table 2 present the empirical power performance of both hypotheses. In both cases we see that the method is well calibrated. For the single hypothesis case, in the upper half of the table, we detect changes in the parameter ν as well as disturbances in the scale matrix. Notably under these alternatives the power is stable throughout different dimensions, since the disturbance only affects the radial part of the distribution. Disturbances in the directional part are also well identified. Dependence and asymmetry are modeled in the multivariate skewed t alternative and are both well detected, although the power of the tests decreases in the asymmetric case when the

dimension increases. For the composite case, in the lower half of the table, the procedure effectively identifies substantial disturbances in the scale matrix; however, small anomalies in the directional component prove to be more challenging to detect. The power behavior under the multivariate skewed t distribution interestingly parallels the simple hypothesis case.

The third part of the simulation study consists of testing for a high-dimensional multivariate stable law for which, to the best of our knowledge, no competing methods exist in the literature. In Table 3, we present the simulation results for testing the multivariate stable distribution for $\beta = 1$ in dimensions $d = 50$ and $d = 100$. Accordingly, the null hypothesis corresponds to $\mathcal{N}_d(\mathbf{0}, \mathbf{I}_d) \otimes [\text{S}(1)]^{1/2}$. It is important to note that there is no numerically stable algorithm for this class of distributions in higher dimensions, see Nolan (2013). The test is able to detect deviations in the context of the multivariate t distribution as the degrees of freedom increase but shows little sensitivity to alternatives with dependence structures, such as DMN. However, when the radial part is also changed to another stable distribution, the power of the test increases, notably in higher dimensions.

	n d	50		100	
		50	100	50	100
$\mathcal{N}_d(\mathbf{0}, \mathbf{I}_d) \otimes [\text{S}(1)]^{1/2}$		5	5	5	5
$t_1(\mathbf{I}_d)$		6	5	5	6
$t_{1.25}(\mathbf{I}_d)$		7	8	13	13
$t_{1.5}(\mathbf{I}_d)$		18	18	42	41
DMN(0) $\otimes [\text{S}(0.8)]^{1/2}$		39	45	69	74
DMN(0.25) $\otimes [\text{S}(0.8)]^{1/2}$		39	44	68	75
DMN(0.5) $\otimes [\text{S}(0.8)]^{1/2}$		38	45	68	74

Table 3: Empirical rejection rates (in percentage) for testing the high-dimensional multivariate stable distribution with $\beta = 1$, here $\mathcal{N}_d(\mathbf{0}, \mathbf{I}_d) \otimes [\text{S}(1)]^{1/2}$.

	n d	100				200			
		100	200	300	1000	100	200	300	1000
vMF(0) $\otimes \Gamma(2, 5)$		5	4	5	6	5	4	4	6
vMF(0.25) $\otimes \chi_2^2$		5	6	5	4	5	5	6	5
vMF(5) $\otimes \chi_d^2$		33	10	6	6	81	22	11	5
vMF(10) $\otimes \chi_{20}^2$		100	56	22	5	100	98	62	6
vMF(2) $\otimes \Gamma(2, 5)$		4	5	5	4	10	5	6	4
vMF(5) $\otimes \Gamma(2, 5)$		33	9	6	5	81	19	10	6
vMF(10) $\otimes \Gamma(2, 5)$		100	57	23	6	100	97	60	7
vMF(20) $\otimes \Gamma(2, 5)$		100	100	99	13	100	100	100	36
vMF(0.25) $\otimes \text{Ca}(2, 5) $		98	98	98	98	100	100	100	100
vMF(0.25) $\otimes t_2 $		47	48	47	48	75	75	75	75

Table 4: Empirical rejection rates (in percentage) for testing the fit to the high-dimensional spherical symmetric distribution with radial part from the gamma family of distributions, both parameters estimated by maximum-likelihood.

Fourth and finally, we present results for the composite case of testing for high-dimensional spherical symmetric distributions with radii following an unknown gamma distribution. The results in Table 4 demonstrate that the procedure, using the bootstrap algorithm with maximum-likelihood estimators for both parameters of the gamma distribution, is well-calibrated. It effectively detects disturbances in the directional component as the concentration parameter of the vMF distribution increases. When examining changes in the radial distribution with only minor disturbances in the

directional component, the power remains consistent across all dimensions, as expected, since the power of the test predominantly arises from the radial component.

5 Discussion

We have derived the asymptotic null distribution for the entire class of Sobolev tests of uniformity on the hypersphere, accommodating arbitrary growth rates of both the dimension and sample size. Additionally, we have characterized the limiting behavior of these tests under a sequence of local alternatives of the integrated von Mises–Fisher type. Our findings have been successfully applied to high-dimensional testing problems involving rotational and spherical symmetry. These results demonstrate that the proposed testing procedures are well-calibrated, maintaining statistical power against both local and fixed alternatives.

The present contribution opens a future line of research on the exhaustive determination of the high-dimensional detection thresholds of Sobolev tests of uniformity against general sequences of rotationally symmetric alternatives, paralleling the development done in the fixed-dimensional case in García-Portugués et al. (2024).

Acknowledgments

The second author acknowledges support from grant PID2021-124051NB-I00, funded by MCIN/-AEI/10.13039/50110001103 and by “ERDF A way of making Europe”. His research was also supported by “Convocatoria de la Universidad Carlos III de Madrid de Ayudas para la recualificación del sistema universitario español para 2021–2023”, funded by Spain’s Ministerio de Ciencia, Innovación y Universidades. The third author acknowledges support from a PDR and a Hubert-Curient grants from the Fonds National de la Recherche Scientifique (FNRS).

References

- Azzalini, A. (2014). *The Skew-Normal and Related Families*. Institute of Mathematical Statistics Monographs. Cambridge University Press, Cambridge.
- Banerjee, A., Dhillon, I. S., Ghosh, J., and Sra, S. (2005). Clustering on the unit hypersphere using von Mises-Fisher distributions. *J. Mach. Learn. Res.*, 6(Sep):1345–1382.
- Beran, R. J. (1968). Testing for uniformity on a compact homogeneous space. *J. Appl. Probab.*, 5(1):177–195.
- Billingsley, P. (2012). *Probability and Measure*. John Wiley & Sons, Hoboken, New Jersey, Anniversary edition.
- Bingham, C. (1974). An antipodally symmetric distribution on the sphere. *Ann. Stat.*, 2(6):1201–1225.
- Bogdan, M., Bogdan, K., and Futschik, A. (2002). A data driven smooth test for circular uniformity. *Ann. Inst. Stat. Math.*, 54(1):29–44.
- Cai, T., Fan, J., and Jiang, T. (2013). Distributions of angles in random packing on spheres. *J. Mach. Learn. Res.*, 14(21):1837–1864.
- Chikuse, Y. (1991). Asymptotic expansions for distributions of the large-sample matrix resultant and related statistics on the Stiefel manifold. *J. Multivar. Anal.*, 39:270–283.

- Chikuse, Y. (1993). High dimensional asymptotic expansions for the matrix Langevin distributions on the Stiefel manifold. *J. Multivar. Anal.*, 44:82–101.
- Cuesta-Albertos, J. A., Cuevas, A., and Fraiman, R. (2009). On projection-based tests for directional and compositional data. *Stat. Comput.*, 19(4):367–380.
- Cutting, C., Paindaveine, D., and Verdebout, T. (2017). Testing uniformity on high-dimensional spheres against monotone rotationally symmetric alternatives. *Ann. Stat.*, 45(3):1024–1058.
- Cutting, C., Paindaveine, D., and Verdebout, T. (2022). Testing uniformity on high-dimensional spheres: The non-null behaviour of the Bingham test. *Ann. Inst. Henri Poincaré Probab. Stat.*, 58(1):567–602.
- DLMF (2020). *NIST Digital Library of Mathematical Functions*. <http://dlmf.nist.gov/>, Release 1.0.27 of 2020-06-15. F. W. J. Olver, A. B. Olde Daalhuis, D. W. Lozier, B. I. Schneider, R. F. Boisvert, C. W. Clark, B. R. Miller and B. V. Saunders, eds.
- Dryden, I. L. (2005). Statistical analysis on high-dimensional spheres and shape spaces. *Ann. Stat.*, 33(4):1643–1665.
- Ebner, B. and Henze, N. (2020). Tests for multivariate normality—a critical review with emphasis on weighted L^2 -statistics. *TEST*, 29(4):845–892.
- Fisher, R. A. (1925). *Statistical Methods for Research Workers*. Oliver and Boyd, Edinburgh.
- García-Portugués, E., Navarro-Esteban, P., and Cuesta-Albertos, J. A. (2023). On a projection-based class of uniformity tests on the hypersphere. *Bernoulli*, 29(1):181–204.
- García-Portugués, E., Paindaveine, D., and Verdebout, T. (2020). On optimal tests for rotational symmetry against new classes of hyperspherical distributions. *J. Am. Stat. Assoc.*, 115(532):1873–1887.
- García-Portugués, E., Paindaveine, D., and Verdebout, T. (2024). On a class of Sobolev tests for symmetry of directions, their detection thresholds, and asymptotic powers. *arXiv:2108.09874v2*.
- García-Portugués, E. and Verdebout, T. (2018). A review of uniformity tests on the hypersphere. *arXiv:1804.00286*.
- Giné, E. (1975). Invariant tests for uniformity on compact Riemannian manifolds based on Sobolev norms. *Ann. Stat.*, 3(6):1243–1266.
- Henze, N. and Wagner, T. (1997). A new approach to the BHEP tests for multivariate normality. *J. Multivar. Anal.*, 62(1):1–23.
- Jupp, P. E. (2008). Data-driven Sobolev tests of uniformity on compact Riemannian manifolds. *Ann. Stat.*, 36(3):1246–1260.
- Jupp, P. E. (2009). Data-driven tests of uniformity on product manifolds. *J. Stat. Plan. Inference*, 139(11):3820–3829.
- Meintanis, S., Milosević, B., Obradović, M., and Veljović, M. (2024). Goodness-of-fit tests for the multivariate Student-t distribution based on i.i.d. data, and for GARCH observations. *J. Time Ser. Anal.*, 45(2):298–319.
- Nolan, J. P. (2013). Multivariate elliptically contoured stable distributions: theory and estimation. *Comput. Stat.*, 28(5):2067–2089.

Paindaveine, D. and Verdebout, T. (2016). On high-dimensional sign tests. *Bernoulli*, 22(3):1745–1769.

Rayleigh, Lord. (1919). On the problem of random vibrations, and of random flights in one, two, or three dimensions. *Lond. Edinb. Dublin Philos. Mag. J. Sci.*, 37(220):321–347.

van der Vaart, A. W. (1998). *Asymptotic Statistics*. Cambridge Series in Statistical and Probabilistic Mathematics. Cambridge University Press, Cambridge.

A Main proofs

Proof of Theorem 2.1. As in Paindaveine and Verdebout (2016, Theorem 2.1), the proof is based on an application of Billingsley (2012)’s (central limit) Theorem 35.12 for martingale difference sequences. For that reason, the theorem is stated as Theorem B.1 in the appendix.

The proof for showing that $\sigma_n^{-1}T_n \rightsquigarrow \mathcal{N}(0, 1)$ is split into checking the three main conditions of Theorem B.1: that T_n has a martingale difference structure, that the variances of the martingale difference terms are finite, and that the Lindeberg condition is satisfied.

Martingale difference structure.

We consider the σ -algebra $\mathcal{F}_{n,\ell} = \sigma(\{\mathbf{X}_{n,1}, \dots, \mathbf{X}_{n,\ell}\})$ that is spanned by the random vectors $\mathbf{X}_{n,1}, \dots, \mathbf{X}_{n,\ell}$ on \mathbb{S}^{d_n} .

It is beneficial to define standardized versions of the kernel ψ and the statistic T_n as

$$\tilde{\psi}_n(x) := \sigma_n^{-1}\psi_n(x) =: \sum_{k=1}^{\infty} \left(1 + \frac{2k}{d_n - 1}\right) \tilde{v}_{k,d_n}^2 C_k^{(d_n-1)/2}(x) \quad \text{and} \quad \tilde{T}_n := \frac{2}{n} \sum_{1 \leq i < j \leq n} \tilde{\psi}_n(\mathbf{X}_{n,i}^\top \mathbf{X}_{n,j}).$$

Under the null hypothesis of uniformity (assumed henceforth), the kernel $\tilde{\psi}_n$ verifies that

$$\mathbb{E} \left[\tilde{\psi}_n(\mathbf{X}_{n,1}^\top \mathbf{X}_{n,2}) \right] = 0 \quad \text{and} \tag{16}$$

$$\mathbb{E} \left[\tilde{\psi}_n(\mathbf{X}_{n,1}^\top \mathbf{X}_{n,2}) \mid \mathbf{X}_{n,1} \right] = 0. \tag{17}$$

Indeed, (16) directly follows from (17) and the latter from

$$\begin{aligned} \mathbb{E} \left[\tilde{\psi}_n(\mathbf{X}_{n,1}^\top \mathbf{X}_{n,2}) \mid \mathbf{X}_{n,1} \right] &= \int_{\mathbb{S}^{d_n}} \tilde{\psi}_n(\mathbf{X}_{n,1}^\top \mathbf{x}_2) \, d\nu_{d_n}(\mathbf{x}_2) \\ &= \frac{1}{\omega_{d_n}} \int_{\mathbb{S}^{d_n-1}} \int_{-1}^1 \tilde{\psi}_n(x)(1-x^2)^{d_n/2-1} \, dx \, d\nu_{d_n-1}(\boldsymbol{\xi}) \\ &= \frac{\omega_{d_n-1}}{\omega_{d_n}} \int_{-1}^1 \sum_{k=1}^{\infty} \left(1 + \frac{2k}{d_n - 1}\right) \tilde{v}_{k,d_n}^2 C_k^{(d_n-1)/2}(x)(1-x^2)^{d_n/2-1} \, dx \\ &= 0, \end{aligned}$$

where ν_{d_n} denotes the uniform measure on \mathbb{S}^{d_n} . Above, we have applied, first, the tangent-normal change of variables $\mathbf{x} = x\boldsymbol{\mu} + (1-x^2)^{1/2}\mathbf{B}_\mu\boldsymbol{\xi}$, for $\mathbf{x}, \boldsymbol{\mu} \in \mathbb{S}^{d_n}$, $x = \mathbf{x}^\top \boldsymbol{\mu}$, $\boldsymbol{\xi} \in \mathbb{S}^{d_n-1}$, and \mathbf{B}_μ a $(d_n+1) \times d_n$ matrix such that $\mathbf{B}_\mu^\top \mathbf{B}_\mu = \mathbf{I}_{d_n}$ and $\mathbf{B}_\mu \mathbf{B}_\mu^\top = \mathbf{I}_{d_n+1} - \boldsymbol{\mu}\boldsymbol{\mu}^\top$; and then the orthogonality of the Gegenbauer polynomials ($C_0^{(d_n-1)/2} \equiv 1$).

We define

$$D_{n,\ell} := \mathbb{E} \left[\tilde{T}_n \mid \mathcal{F}_{n,\ell} \right] - \mathbb{E} \left[\tilde{T}_n \mid \mathcal{F}_{n,\ell-1} \right], \quad \ell = 1, \dots, n, \quad n = 1, 2, \dots, \tag{18}$$

which, by definition, is a martingale difference sequence. The form of $D_{n,\ell}$ is determined by computing $\mathbb{E}[\tilde{T}_n | \mathcal{F}_{n,\ell}]$ next. Throughout, sums over empty sets of indices are defined as being equal to zero. We have that

$$\begin{aligned}
\frac{n}{2}\mathbb{E}[\tilde{T}_n | \mathcal{F}_{n,\ell}] &= \sum_{i=1}^{n-1} \sum_{j=i+1}^n \mathbb{E}[\tilde{\psi}_n(\mathbf{X}_{n,i}^\top \mathbf{X}_{n,j}) | \mathcal{F}_{n,\ell}] \\
&= \sum_{i=1}^{\ell-1} \sum_{j=i+1}^{\ell-1} \mathbb{E}[\tilde{\psi}_n(\mathbf{X}_{n,i}^\top \mathbf{X}_{n,j}) | \mathbf{X}_{n,i}, \mathbf{X}_{n,j}] \\
&\quad + \sum_{i=1}^{\ell-1} \mathbb{E}[\tilde{\psi}_n(\mathbf{X}_{n,i}^\top \mathbf{X}_{n,\ell}) | \mathbf{X}_{n,i}, \mathbf{X}_{n,\ell}] + \sum_{i=1}^{\ell-1} \sum_{j=\ell+1}^{n-1} \mathbb{E}[\tilde{\psi}_n(\mathbf{X}_{n,i}^\top \mathbf{X}_{n,j}) | \mathbf{X}_{n,i}] \\
&\quad + \sum_{j=\ell+1}^n \mathbb{E}[\tilde{\psi}_n(\mathbf{X}_{n,\ell}^\top \mathbf{X}_{n,j}) | \mathbf{X}_{n,\ell}] + \sum_{i=\ell+1}^{n-1} \sum_{j=i+1}^n \mathbb{E}[\tilde{\psi}_n(\mathbf{X}_{n,i}^\top \mathbf{X}_{n,j}) | \mathbf{X}_{n,1}, \dots, \mathbf{X}_{n,\ell}] \\
&= \sum_{i=1}^{\ell-1} \sum_{j=i+1}^{\ell-1} \tilde{\psi}_n(\mathbf{X}_{n,i}^\top \mathbf{X}_{n,j}) + \sum_{i=1}^{\ell-1} \tilde{\psi}_n(\mathbf{X}_{n,i}^\top \mathbf{X}_{n,\ell}) \\
&= \sum_{i=1}^{\ell-1} \sum_{j=i+1}^{\ell} \tilde{\psi}_n(\mathbf{X}_{n,i}^\top \mathbf{X}_{n,j}),
\end{aligned}$$

where we have used (16) and (17). Therefore,

$$\begin{aligned}
\frac{n}{2}D_{n,\ell} &= \frac{n}{2} \left(\mathbb{E}[\tilde{T}_n | \mathcal{F}_{n,\ell}] - \mathbb{E}[\tilde{T}_n | \mathcal{F}_{n,\ell-1}] \right) \\
&= \sum_{i=1}^{\ell-1} \sum_{j=i+1}^{\ell} \tilde{\psi}_n(\mathbf{X}_{n,i}^\top \mathbf{X}_{n,j}) - \sum_{i=1}^{\ell-2} \sum_{j=i+1}^{\ell-1} \tilde{\psi}_n(\mathbf{X}_{n,i}^\top \mathbf{X}_{n,j}) \\
&= \tilde{\psi}_n(\mathbf{X}_{n,\ell-1}^\top \mathbf{X}_{n,\ell}) + \sum_{i=1}^{\ell-2} \sum_{j=i+1}^{\ell} \tilde{\psi}_n(\mathbf{X}_{n,i}^\top \mathbf{X}_{n,j}) - \sum_{i=1}^{\ell-2} \sum_{j=i+1}^{\ell-1} \tilde{\psi}_n(\mathbf{X}_{n,i}^\top \mathbf{X}_{n,j}) \\
&= \sum_{i=1}^{\ell-1} \tilde{\psi}_n(\mathbf{X}_{n,i}^\top \mathbf{X}_{n,\ell}).
\end{aligned}$$

In particular, we have that $D_{n,1} = 0$. Hence,

$$\tilde{T}_n = \frac{2}{n} \sum_{1 \leq i < j \leq n} \tilde{\psi}_n(\mathbf{X}_{n,i}^\top \mathbf{X}_{n,j}) = \frac{2}{n} \sum_{j=2}^n \sum_{i=1}^{j-1} \tilde{\psi}_n(\mathbf{X}_{n,i}^\top \mathbf{X}_{n,j}) = \sum_{j=2}^n D_{n,\ell} = \sum_{j=1}^n D_{n,\ell}$$

and \tilde{T}_n has a martingale difference structure.

Finite variance of $D_{n,\ell}$.

First, observe that $\tilde{\psi}_n(\mathbf{X}_{n,i}^\top \mathbf{X}_{n,\ell})$ and $\tilde{\psi}_n(\mathbf{X}_{n,j}^\top \mathbf{X}_{n,\ell})$ are uncorrelated for $i \neq j$ and $1 \leq i, j < \ell$ since

$$\mathbb{E}[\tilde{\psi}_n(\mathbf{X}_{n,i}^\top \mathbf{X}_{n,\ell}) \tilde{\psi}_n(\mathbf{X}_{n,j}^\top \mathbf{X}_{n,\ell})] = \mathbb{E}[\mathbb{E}[\tilde{\psi}_n(\mathbf{X}_{n,i}^\top \mathbf{X}_{n,\ell}) | \mathbf{X}_{n,\ell}] \mathbb{E}[\tilde{\psi}_n(\mathbf{X}_{n,j}^\top \mathbf{X}_{n,\ell}) | \mathbf{X}_{n,\ell}]] = 0$$

because of (16). We then have that

$$\text{Var}[D_{n,\ell}] = \frac{4}{n^2} \sum_{i=1}^{\ell-1} \text{Var}[\tilde{\psi}_n(\mathbf{X}_{n,i}^\top \mathbf{X}_{n,\ell})] = \frac{4}{n^2} (\ell-1) \mathbb{E}[\tilde{\psi}_n^2(\mathbf{X}_{n,1}^\top \mathbf{X}_{n,2})].$$

Because of the definition of σ_n^2 in (6),

$$\mathbb{E} \left[\tilde{\psi}_n^2(\mathbf{X}_{n,1}^\top \mathbf{X}_{n,2}) \right] = \frac{\mathbb{E}[\psi_n^2(\mathbf{X}_{n,1}^\top \mathbf{X}_{n,2})]}{\sigma_n^2} = \frac{1}{2} \quad (19)$$

and hence

$$\text{Var} [D_{n,\ell}] = \frac{2}{n^2}(\ell - 1) < \infty. \quad (20)$$

Convergence of $\sum_{\ell=1}^n \sigma_{n,\ell}^2$ to 1 in probability.

We show that $\sum_{\ell=1}^n \sigma_{n,\ell}^2$ converges to 1 in mean square, where $\sigma_{n,\ell}^2 := \mathbb{E}[D_{n,\ell}^2 \mid \mathcal{F}_{n,\ell-1}]$. For that, we show that $\mathbb{E}[\sum_{\ell=1}^n \sigma_{n,\ell}^2] \rightarrow 1$ and $\text{Var}[\sum_{\ell=1}^n \sigma_{n,\ell}^2] \rightarrow 0$.

First, note that

$$\begin{aligned} \sigma_{n,\ell}^2 &= \mathbb{E} [D_{n,\ell}^2 \mid \mathcal{F}_{n,\ell-1}] \\ &= \frac{4}{n^2} \sum_{i=1}^{\ell-1} \mathbb{E} \left[\tilde{\psi}_n^2(\mathbf{X}_{n,i}^\top \mathbf{X}_{n,\ell}) \mid \mathbf{X}_{n,i} \right] + \frac{4}{n^2} \sum_{1 \leq i \neq j \leq \ell-1} \mathbb{E} \left[\tilde{\psi}_n(\mathbf{X}_{n,i}^\top \mathbf{X}_{n,\ell}) \tilde{\psi}_n(\mathbf{X}_{n,j}^\top \mathbf{X}_{n,\ell}) \mid \mathbf{X}_{n,i}, \mathbf{X}_{n,j} \right] \\ &= \frac{4}{n^2} \frac{\ell-1}{2} + \frac{8}{n^2} \sum_{1 \leq i < j \leq \ell-1} \mathbb{E} \left[\tilde{\psi}_n(\mathbf{X}_{n,i}^\top \mathbf{X}_{n,\ell}) \tilde{\psi}_n(\mathbf{X}_{n,j}^\top \mathbf{X}_{n,\ell}) \mid \mathbf{X}_{n,i}, \mathbf{X}_{n,j} \right] \end{aligned} \quad (21)$$

because

$$\mathbb{E} \left[\tilde{\psi}_n^2(\mathbf{X}_{n,i}^\top \mathbf{X}_{n,\ell}) \mid \mathbf{X}_{n,i} \right] = \omega_{d_n-1} \int_{-1}^1 \tilde{\psi}_n^2(x) (1-x^2)^{d_n/2-1} dx = \mathbb{E} \left[\tilde{\psi}_n^2(\mathbf{X}_{n,i}^\top \mathbf{X}_{n,\ell}) \right] = \frac{1}{2}.$$

Then, from (21) and (19),

$$\mathbb{E} [\sigma_{n,\ell}^2] = \frac{2(\ell-1)}{n^2}$$

since, for $i \neq j$ and $1 \leq i, j \leq \ell-1$, $\mathbb{E}[\tilde{\psi}_n(\mathbf{X}_{n,i}^\top \mathbf{X}_{n,\ell}) \tilde{\psi}_n(\mathbf{X}_{n,j}^\top \mathbf{X}_{n,\ell})] = \mathbb{E}[\tilde{\psi}_n(\mathbf{X}_{n,i}^\top \mathbf{X}_{n,\ell}) \mid \mathbf{X}_{n,i}] \cdot \mathbb{E}[\tilde{\psi}_n(\mathbf{X}_{n,j}^\top \mathbf{X}_{n,\ell}) \mid \mathbf{X}_{n,j}] = 0$ by (17). It therefore follows that

$$\mathbb{E} \left[\sum_{\ell=1}^n \sigma_{n,\ell}^2 \right] = \frac{2}{n^2} \sum_{\ell=1}^n (\ell-1) = \frac{2}{n^2} \sum_{\ell=1}^{n-1} \ell = \frac{2}{n^2} \frac{(n-1)n}{2} = \frac{n-1}{n} \rightarrow 1$$

as $n \rightarrow \infty$.

Now, from (21), we have that

$$\begin{aligned} \text{Var} \left[\sum_{\ell=1}^n \sigma_{n,\ell}^2 \right] &= \frac{64}{n^4} \text{Var} \left[\sum_{\ell=3}^n \sum_{1 \leq i < j \leq \ell-1} \mathbb{E} \left[\tilde{\psi}_n(\mathbf{X}_{n,i}^\top \mathbf{X}_{n,\ell}) \tilde{\psi}_n(\mathbf{X}_{n,j}^\top \mathbf{X}_{n,\ell}) \mid \mathbf{X}_{n,i}, \mathbf{X}_{n,j} \right] \right] \\ &= \frac{64}{n^4} \text{Var} \left[\sum_{1 \leq i < j \leq n} (n-j) \mathbb{E} \left[\tilde{\psi}_n(\mathbf{X}_{n,i}^\top \mathbf{X}_{n,\ell}) \tilde{\psi}_n(\mathbf{X}_{n,j}^\top \mathbf{X}_{n,\ell}) \mid \mathbf{X}_{n,i}, \mathbf{X}_{n,j} \right] \right] \end{aligned} \quad (22)$$

$$=: \frac{64}{n^4} \text{Var} \left[\sum_{1 \leq i < j \leq n} (n-j) f_{ij} \right], \quad (23)$$

where in (22) we have used that $\sum_{\ell=3}^n \sum_{1 \leq i < j \leq \ell-1} c_{ij} = \sum_{1 \leq i < j \leq n-1} (n+1-j) c_{ij} = \sum_{1 \leq i < j \leq n} (n-j) c_{ij}$. The $\{f_{ij}\}_{1 \leq i < j \leq n}$ are pairwise uncorrelated, since

$$\mathbb{E} [f_{12} \mid \mathbf{X}_{n,1}] = \mathbb{E} \left[\tilde{\psi}_n(\mathbf{X}_{n,1}^\top \mathbf{X}_{n,\ell}) \tilde{\psi}_n(\mathbf{X}_{n,2}^\top \mathbf{X}_{n,\ell}) \mid \mathbf{X}_{n,1} \right]$$

$$= \mathbb{E} \left[\tilde{\psi}_n(\mathbf{X}_{n,1}^\top \mathbf{X}_{n,\ell}) \mathbb{E} \left[\tilde{\psi}_n(\mathbf{X}_{n,2}^\top \mathbf{X}_{n,\ell} \mid \mathbf{X}_{n,\ell}) \mid \mathbf{X}_{n,1} \right] \right] = 0$$

and therefore $\mathbb{E}[f_{12}f_{13}] = \mathbb{E}[\mathbb{E}[f_{12} \mid \mathbf{X}_{n,1}] \mathbb{E}[f_{13} \mid \mathbf{X}_{n,1}]] = 0$ and $\mathbb{E}[f_{12}] = 0$. Hence, (23) becomes

$$\begin{aligned} \text{Var} \left[\sum_{\ell=1}^n \sigma_{n,\ell}^2 \right] &= \frac{64}{n^4} \sum_{1 \leq i < j \leq n} (n-j)^2 \text{Var}[f_{ij}] \\ &= \frac{64}{n^4} \mathbb{E}[f_{12}^2] \sum_{1 \leq i < j \leq n} (n-j)^2. \end{aligned}$$

Now,

$$\sum_{1 \leq i < j \leq n} (n-j)^2 = \sum_{j=2}^n (j-1)(n-j)^2 = \sum_{j=1}^{n-1} j(n-j-1)^2 \leq n^2 \sum_{j=1}^{n-1} j = \frac{n^3(n-1)}{2},$$

which gives

$$\text{Var} \left[\sum_{\ell=1}^n \sigma_{n,\ell}^2 \right] \leq \frac{64}{n^4} \mathbb{E}[f_{12}^2] \frac{n^3(n-1)}{2} = \frac{32(n-1)}{n} \mathbb{E}[f_{12}^2].$$

Exploiting the definition (5) of the kernel $\tilde{\psi}_n$ in terms of a mean square convergent series, we can get express $\mathbb{E}[f_{ij}^2]$ throughout the coefficients of ψ_n :

$$\begin{aligned} &\mathbb{E} \left[\tilde{\psi}_n(\mathbf{X}_{n,i}^\top \mathbf{X}_{n,\ell}) \tilde{\psi}_n(\mathbf{X}_{n,j}^\top \mathbf{X}_{n,\ell}) \mid \mathbf{X}_{n,i}, \mathbf{X}_{n,j} \right] \\ &= \int_{\mathbb{S}^{d_n}} \tilde{\psi}_n(\mathbf{X}_{n,i}^\top \mathbf{x}) \tilde{\psi}_n(\mathbf{X}_{n,j}^\top \mathbf{x}) \, d\nu_{d_n}(\mathbf{x}) \\ &= \sum_{k_1, k_2=1}^{\infty} \left(1 + \frac{2k_1}{d_n - 1}\right) \left(1 + \frac{2k_2}{d_n - 1}\right) \tilde{v}_{k_1, d_n}^2 \tilde{v}_{k_2, d_n}^2 \int_{\mathbb{S}^{d_n}} C_{k_1}^{(d_n-1)/2}(\mathbf{X}_{n,i}^\top \mathbf{x}) C_{k_2}^{(d_n-1)/2}(\mathbf{X}_{n,j}^\top \mathbf{x}) \, d\nu_{d_n}(\mathbf{x}) \\ &= \sum_{k=1}^{\infty} \left(1 + \frac{2k}{d_n - 1}\right)^2 \tilde{v}_{k, d_n}^4 \left(1 + \frac{2k}{d_n - 1}\right)^{-1} C_k^{(d_n-1)/2}(\mathbf{X}_{n,i}^\top \mathbf{X}_{n,j}) \tag{24} \\ &= \sum_{k=1}^{\infty} \left(1 + \frac{2k}{d_n - 1}\right) \tilde{v}_{k, d_n}^4 C_k^{(d_n-1)/2}(\mathbf{X}_{n,i}^\top \mathbf{X}_{n,j}), \end{aligned}$$

with equality (24) following, e.g., from Lemma B.7 in the Supplementary Material of García-Portugués et al. (2023). Then, due to the orthogonality of Gegenbauer polynomials,

$$\begin{aligned} \mathbb{E}[f_{ij}^2] &= \mathbb{E} \left[\left\{ \sum_{k=1}^{\infty} \left(1 + \frac{2k}{d_n - 1}\right) \tilde{v}_{k, d_n}^4 C_k^{(d_n-1)/2}(\mathbf{X}_{n,i}^\top \mathbf{X}_{n,j}) \right\}^2 \right] \\ &= \mathbb{E} \left[\sum_{k=1}^{\infty} \left(1 + \frac{2k}{d_n - 1}\right)^2 \tilde{v}_{k, d_n}^8 \left(C_k^{(d_n-1)/2}(\mathbf{X}_{n,i}^\top \mathbf{X}_{n,j}) \right)^2 \right] \\ &= \sum_{k=1}^{\infty} \left(1 + \frac{2k}{d_n - 1}\right)^2 \tilde{v}_{k, d_n}^8 \frac{\omega_{d_n-1}}{\omega_{d_n}} c_{k, d_n}, \tag{25} \end{aligned}$$

with c_{k, d_n} defined in (2). Due to (3), (25) becomes

$$\mathbb{E}[f_{ij}^2] = \sum_{k=1}^{\infty} \tilde{v}_{k, d_n}^8 d_{k, d_n} = \frac{\sum_{k=1}^{\infty} v_{k, d_n}^8 d_{k, d_n}}{4 \mathbb{E}[\psi_n^2(\mathbf{X}_{n,1}^\top \mathbf{X}_{n,2})]} = \frac{\sum_{k=1}^{\infty} v_{k, d_n}^8 d_{k, d_n}}{4 \left(\sum_{k=1}^{\infty} v_{k, d_n}^4 d_{k, d_n} \right)^2}.$$

Therefore,

$$\text{Var} \left[\sum_{\ell=1}^n \sigma_{n,\ell}^2 \right] \leq \frac{32(n-1)}{n} \mathbb{E} [f_{12}^2] = \frac{8(n-1)}{n} \frac{\sum_{k=1}^{\infty} v_{k,d_n}^8 d_{k,d_n}}{(\sum_{k=1}^{\infty} v_{k,d_n}^4 d_{k,d_n})^2} = o(1) \quad (26)$$

by condition (7).

Alternatively to (26), by Jensen and Cauchy–Schwartz inequalities, for $1 \leq i < j \leq \ell - 1$,

$$\begin{aligned} \mathbb{E} [f_{ij}^2] &= \mathbb{E} \left[\mathbb{E} [\tilde{\psi}_n(\mathbf{X}_{n,i}^\top \mathbf{X}_{n,\ell}) \tilde{\psi}_n(\mathbf{X}_{n,j}^\top \mathbf{X}_{n,\ell}) \mid \mathbf{X}_{n,i}, \mathbf{X}_{n,j}]^2 \right] \\ &\leq \mathbb{E} \left[\mathbb{E} [\tilde{\psi}_n^2(\mathbf{X}_{n,i}^\top \mathbf{X}_{n,\ell}) \tilde{\psi}_n^2(\mathbf{X}_{n,j}^\top \mathbf{X}_{n,\ell}) \mid \mathbf{X}_{n,i}, \mathbf{X}_{n,j}] \right] \\ &\leq \mathbb{E} \left[\sqrt{\mathbb{E} [\tilde{\psi}_n^4(\mathbf{X}_{n,i}^\top \mathbf{X}_{n,\ell}) \mid \mathbf{X}_{n,i}] \mathbb{E} [\tilde{\psi}_n^4(\mathbf{X}_{n,j}^\top \mathbf{X}_{n,\ell}) \mid \mathbf{X}_{n,j}]} \right] \\ &= \mathbb{E} \left[\tilde{\psi}_n^4(\mathbf{X}_{n,1}^\top \mathbf{X}_{n,2}) \right] \\ &= \frac{\mathbb{E} [\psi_n^4(\mathbf{X}_{n,1}^\top \mathbf{X}_{n,2})]}{4\mathbb{E} [\psi_n^2(\mathbf{X}_{n,1}^\top \mathbf{X}_{n,2})]^2}. \end{aligned}$$

Therefore, condition (8) is implied by condition (7) and Remark 2.1 follows.

Lindeberg condition.

By the Cauchy–Schwartz and Chebyshev inequalities, and then (20), we have

$$\begin{aligned} \sum_{\ell=1}^n \mathbb{E} \left[D_{n,\ell}^2 \mathbf{1}_{\{|D_{n,\ell}| > \varepsilon\}} \right] &\leq \sum_{\ell=1}^n \sqrt{\mathbb{E} [D_{n,\ell}^4]} \sqrt{\mathbb{P} [|D_{n,\ell}| > \varepsilon]} \\ &\leq \frac{1}{\varepsilon} \sum_{\ell=1}^n \sqrt{\mathbb{E} [D_{n,\ell}^4]} \sqrt{\text{Var} [D_{n,\ell}]} \\ &= \frac{\sqrt{2}}{\varepsilon n} \sum_{\ell=1}^n \sqrt{\mathbb{E} [D_{n,\ell}^4]} \sqrt{\ell - 1}. \end{aligned} \quad (27)$$

The fourth moment of $D_{n,\ell}$ is

$$\begin{aligned} \mathbb{E} [D_{n,\ell}^4] &= \frac{16}{n^4} \mathbb{E} \left[\left(\sum_{i=1}^{\ell-1} \tilde{\psi}_n(\mathbf{X}_{n,i}^\top \mathbf{X}_{n,\ell}) \right)^4 \right] \\ &= \frac{16}{n^4} \sum_{i_1, i_2, i_3, i_4=1}^{\ell-1} \mathbb{E} \left[\tilde{\psi}_n(\mathbf{X}_{n,i_1}^\top \mathbf{X}_{n,\ell}) \tilde{\psi}_n(\mathbf{X}_{n,i_2}^\top \mathbf{X}_{n,\ell}) \tilde{\psi}_n(\mathbf{X}_{n,i_3}^\top \mathbf{X}_{n,\ell}) \tilde{\psi}_n(\mathbf{X}_{n,i_4}^\top \mathbf{X}_{n,\ell}) \right] \\ &= \frac{16}{n^4} \left\{ (\ell-1) \mathbb{E} \left[\tilde{\psi}_n^4(\mathbf{X}_{n,1}^\top \mathbf{X}_{n,\ell}) \right] + 3(\ell-1)(\ell-2) \mathbb{E} \left[\tilde{\psi}_n^2(\mathbf{X}_{n,1}^\top \mathbf{X}_{n,\ell}) \right]^2 \right\} \\ &= \frac{16(\ell-1)}{n^4} \left\{ \mathbb{E} \left[\tilde{\psi}_n^4(\mathbf{X}_{n,1}^\top \mathbf{X}_{n,\ell}) \right] + 3(\ell-2) \right\} \end{aligned} \quad (28)$$

with (28) following because of (16) and (17), which makes other terms null (e.g., due to (17), $\mathbb{E} [\tilde{\psi}_n(\mathbf{X}_{n,1}^\top \mathbf{X}_{n,\ell}) \tilde{\psi}_n^3(\mathbf{X}_{n,2}^\top \mathbf{X}_{n,\ell})] = 0$). Since $\mathbb{E} [\tilde{\psi}_n^4(\mathbf{X}_{n,1}^\top \mathbf{X}_{n,\ell})] = O(1)$ as $n \rightarrow \infty$ and $d_n \rightarrow \infty$ by condition (7), then

$$\mathbb{E} [D_{n,\ell}^4] \leq \frac{16(\ell-1)^2}{n^4} \{C + 3\} \quad (29)$$

for $C > 0$ independent of n .

Replacing (29) in (27) results in

$$\begin{aligned}
\sum_{\ell=1}^n \mathbb{E} \left[D_{n,\ell}^2 1_{\{|D_{n,\ell}| > \varepsilon\}} \right] &\leq \frac{\sqrt{2}}{\varepsilon n} \sum_{\ell=1}^n \sqrt{\frac{16(\ell-1)^2(C+3)}{n^4}} \sqrt{\ell-1} \\
&= \frac{4\sqrt{2(C+3)}}{\varepsilon n^3} \sum_{\ell=1}^n (\ell-1)^{3/2} \\
&= \frac{4\sqrt{2(C+3)}}{\varepsilon n^3} O(n^{5/2}) \\
&= \frac{1}{\varepsilon} O(n^{-1/2}),
\end{aligned}$$

and hence the Lindeberg condition is also satisfied. \square

Proof of Theorem 2.2. It directly follows from Theorem 4.2 in Cutting et al. (2017) that the sequence of integrated von Mises–Fisher models with concentration κ_n is locally and asymptotically normal with central sequence

$$\Delta_{n,\ell} := \frac{\sqrt{d_n}}{\sqrt{2}n} \sum_{i=1}^{\ell-1} \mathbf{X}_{n,i}^\top \mathbf{X}_{n,\ell}$$

and Fisher information $\Sigma = 1/2$. Under the null hypothesis, a direct application of the Cramér–Wold theorem entails that $\mathbf{T}_n := \sum_{\ell=1}^n (D_{n,\ell}, \Delta_{n,\ell})^\top$ (with $D_{n,\ell}$ as in (18) in the proof of Theorem 2.1) is asymptotically bivariate normal with mean zero and covariance matrix

$$\begin{pmatrix} 1 & \Gamma \\ \Gamma & \Sigma \end{pmatrix},$$

where, due to the pairwise independence of the $\mathbf{X}_{n,i}^\top \mathbf{X}_{n,j}$'s and the orthogonality of the Gegenbauer polynomials,

$$\begin{aligned}
\Gamma &= \lim_{n \rightarrow \infty} \frac{2\sqrt{d_n}}{n^2} \sum_{\ell, \ell'=1}^n \sum_{j=1}^{\ell-1} \sum_{i=1}^{\ell'-1} \text{Cov}(\tilde{\psi}_n(\mathbf{X}_{n,i}^\top \mathbf{X}_{n,\ell'}), \mathbf{X}_{n,j}^\top \mathbf{X}_{n,\ell}) \\
&= \lim_{n \rightarrow \infty} \frac{2\sqrt{d_n}}{n^2} \sum_{\ell, \ell'=1}^n \sum_{j=1}^{\ell-1} \sum_{i=1}^{\ell'-1} \mathbb{E} \left[\tilde{\psi}_n(\mathbf{X}_{n,i}^\top \mathbf{X}_{n,\ell'}) \mathbf{X}_{n,j}^\top \mathbf{X}_{n,\ell} \right] \\
&= \lim_{n \rightarrow \infty} \frac{2\sqrt{d_n}}{n^2} \sum_{\ell, \ell'=1}^n \sum_{j=1}^{\ell-1} \sum_{i=1}^{\ell'-1} \sum_{k=1}^{\infty} \left(1 + \frac{2k}{d_n - 1} \right) \tilde{v}_{k,d_n}^2 \mathbb{E} \left[C_k^{(d_n-1)/2} (\mathbf{X}_{n,i}^\top \mathbf{X}_{n,\ell'}) \mathbf{X}_{n,j}^\top \mathbf{X}_{n,\ell} \right] \\
&= \lim_{n \rightarrow \infty} \frac{n(n-1) \left((d_n-1) + 2 \right) \sqrt{d_n} \tilde{v}_{1,d_n}^2}{n^2} \mathbb{E} \left[(\mathbf{X}_{n,1}^\top \mathbf{X}_{n,2})^2 \right] \\
&= \lim_{n \rightarrow \infty} \frac{n(n-1) \left((d_n-1) + 2 \right) \sqrt{d_n} v_{1,d_n}^2}{n^2 d_n \sigma_n} \\
&= \lim_{n \rightarrow \infty} \frac{\sqrt{d_n} v_{1,d_n}^2}{\sqrt{2} \left(\sum_{k=1}^{\infty} v_{k,d_n}^4 d_{k,d_n} \right)^{1/2}}.
\end{aligned}$$

The result then follows from a direct application of the third Le Cam Lemma (see Theorem 6.6 in van der Vaart, 1998). \square

B Required results

Theorem B.1 (Theorem 35.12 in Billingsley (2012)). *Let $D_{n,\ell}$, $\ell = 1, \dots, n$, $n = 1, 2, \dots$, be a triangular array of random variables such that, for any n , $D_{n,1}, \dots, D_{n,n}$ is a martingale difference sequence with respect to some filtration $\mathcal{F}_{n,1}, \dots, \mathcal{F}_{n,n}$. Assume that $\text{Var}[D_{n,\ell}] < \infty$ for any (n, ℓ) . Letting $\sigma_{n,\ell}^2 := \mathbb{E}[D_{n,\ell}^2 \mid \mathcal{F}_{n,\ell-1}]$ (with $\mathcal{F}_{n,0}$ being the trivial σ -algebra $\{\emptyset, \Omega\}$ for all n), further assume that*

$$\sum_{\ell=1}^n \sigma_{n,\ell}^2 \xrightarrow{\mathbb{P}} 1$$

as $n \rightarrow \infty$ and the Lindeberg condition

$$\sum_{\ell=1}^n \mathbb{E} \left[D_{n,\ell}^2 1_{\{|D_{n,\ell}| > \varepsilon\}} \right] \rightarrow 0 \quad \text{for all } \varepsilon > 0 \text{ as } n \rightarrow \infty.$$

Then $\sum_{\ell=1}^n D_{n,\ell} \rightsquigarrow \mathcal{N}(0, 1)$.

Lemma B.1. *Let $\mathbf{X}_{n,1}$ and $\mathbf{X}_{n,2}$ be two independent random vectors uniformly distributed on \mathbb{S}^{d_n} . For any integers $k, m \geq 1$,*

$$\mathbb{E} \left[\left\{ C_k^{(d_n-1)/2}(\mathbf{X}_{n,1}^\top \mathbf{X}_{n,2}) \right\}^{2m} \right] \asymp d_n^{mk} \quad \text{and} \quad d_{k,d_n} \sim \left(1 + \frac{2k}{d_n - 1} \right) \frac{d_n^k}{k!} \quad \text{as } d_n \rightarrow \infty,$$

with $a_n \asymp b_n$ denoting that $a_n/b_n \rightarrow c \neq 0$ as $n \rightarrow \infty$, and $a_n \sim b_n$ that $a_n/b_n \rightarrow 1$ as $n \rightarrow \infty$.

Proof of Lemma B.1. On the one hand, due to Equation 18.5.10 in DLMF (2020),

$$C_k^{(d_n-1)/2}(x) = \sum_{\ell=0}^{\lfloor k/2 \rfloor} \frac{(-1)^\ell 2^{k-2\ell} ((d_n-1)/2)_{k-\ell}}{\ell!(k-2\ell)!} x^{k-2\ell} =: \sum_{\ell=0}^{\lfloor k/2 \rfloor} a_{k,\ell,d_n} x^{k-2\ell},$$

where $(a)_k := \Gamma(a+k)/\Gamma(a)$ is the Pochhammer symbol. The coefficients a_{k,ℓ,d_n} , $\ell = 0, \dots, \lfloor k/2 \rfloor$, are such that

$$a_{k,\ell,d_n} = a_{k,\ell} \left(\frac{d_n-1}{2} \right)_{k-\ell} = a_{k,\ell} \frac{\Gamma\left(\frac{d_n-1}{2} + k - \ell\right)}{\Gamma\left(\frac{d_n-1}{2}\right)} \sim a_{k,\ell} \left(\frac{d_n-1}{2} + k - \ell \right)^{k-\ell} = O(d_n^{k-\ell}), \quad (30)$$

where $a_{k,\ell}$ is a constant independent from d_n and we have used Lemma B.3 in the Supplementary Material of García-Portugués et al. (2023): if $a \geq b$ and $\gamma > 0$, then $\Gamma(\gamma d + a)/\Gamma(\gamma d + b) \sim (\gamma d + a)^{a-b}$ as $d \rightarrow \infty$.

On the other hand, from Lemma A.1 in Paindaveine and Verdebout (2016), we have that

$$\mathbb{E} \left[(\mathbf{X}_{n,1}^\top \mathbf{X}_{n,2})^{2m} \right] = \prod_{r=0}^{m-1} \frac{1+2r}{d_n+1+2r} = O(d_n^{-m}). \quad (31)$$

Joining (30) and (31) gives

$$\begin{aligned} \mathbb{E} \left[\left\{ C_k^{(d_n-1)/2}(\mathbf{X}_{n,1}^\top \mathbf{X}_{n,2}) \right\}^{2m} \right] &= \sum_{\ell_1, \dots, \ell_{2m}=0}^{\lfloor k/2 \rfloor} \left\{ \prod_{j=1}^{2m} a_{k,\ell_j,d_n} \right\} \mathbb{E} \left[(\mathbf{X}_{n,1}^\top \mathbf{X}_{n,2})^{2mk-2\sum_{j=1}^{2m} \ell_j} \right] \\ &= \sum_{\ell_1, \dots, \ell_{2m}=0}^{\lfloor k/2 \rfloor} O\left(d_n^{2mk-\sum_{j=1}^{2m} \ell_j}\right) O\left(d_n^{-(mk-\sum_{j=1}^{2m} \ell_j)}\right) \\ &= O\left(d_n^{-mk}\right). \end{aligned}$$

Finally, (4) and the previous asymptotic gamma expansion yield

$$d_{k,d_n} = \left(1 + \frac{2k}{d_n - 1}\right) \frac{\Gamma(d_n - 1 + k)}{\Gamma(d_n - 1)k!} \sim \left(1 + \frac{2k}{d_n - 1}\right) \frac{d_n^k}{k!} \asymp d_n^k.$$

□

C Numerical experiments illustrating Theorems 2.1 and 2.2

We conduct some numerical experiments to empirically evaluate the convergence of the test statistic $\sigma_n^{-1}T_n$ towards the asymptotic distributions stated in Theorems 2.1 and 2.2 when $n \rightarrow \infty$ and $d_n \rightarrow \infty$.

First, we considered k_0 -Sobolev tests given by the sequence of weights $v_{k,d_n} = \delta_{k,k_0}$, for a fixed $k_0 \geq 1$. Under $\mathcal{H}_{0,n}$, as given in (9), we have

$$\tilde{T}_{n,k_0} := \frac{\sqrt{2k_0!}}{d_n^{k_0/2}n} \sum_{1 \leq i < j \leq n} C_{k_0}^{(d_n-1)/2}(\mathbf{X}_{n,i}^\top \mathbf{X}_{n,j}) \rightsquigarrow \mathcal{N}(0, 1). \quad (32)$$

We simulated $M = 10,000$ Monte Carlo samples $\mathbf{X}_{1,n}, \dots, \mathbf{X}_{n,n}$ uniformly distributed on \mathbb{S}^{d_n} for the pairs $(n, d_n) \in \{5, 50, 100, 500\}^2$. Figures 1–2 show the histograms of sample realizations of \tilde{T}_{n,k_0} for $k_0 = 1, 3$, respectively for varying (n, d_n) . The plots show that the histograms and the kernel density estimators (black curve) converge to the density of a $\mathcal{N}(0, 1)$ (blue curve) as $\min(n, d_n) \rightarrow \infty$. The Kolmogorov–Smirnov (KS) test for a $\mathcal{N}(0, 1)$ and the Lilliefors (L) test of normality are conducted to verify the convergence towards the limit distribution, and their p -values are reported for each scenario. For both figures, the p -values increasingly separate from zero as $\min(n, d_n)$ grows, considering that each p -value is asymptotically an independent uniform random variable.

Second, we repeated the same experiment for k_0 -Sobolev tests, but now with samples $\mathbf{X}_{n,1}, \dots, \mathbf{X}_{n,n}$ simulated under $\mathcal{H}_{1,n}$ defined by an integrated von Mises–Fisher distribution (10) on \mathbb{S}^{d_n} with concentration $\kappa_n = \tau d_n^{3/4} / \sqrt{n}$ for $\tau > 0$. According to Theorem 2.2 and subsequent comments, (32) becomes

$$\tilde{T}_{n,k_0} \rightsquigarrow \mathcal{N}(\Gamma\tau^2, 1)$$

under $\mathcal{H}_{1,n}$, with $\Gamma = (1/\sqrt{2})1_{\{k_0=1\}}$. Setting $\tau^2 = \sqrt{2}$ yields the asymptotic non-null distribution $\mathcal{N}(1_{\{k_0=1\}}, 1)$. Figure 3 shows the convergence of the histogram and kernel density estimator of the sample realizations of \tilde{T}_{n,k_0} for $k_0 = 1$ toward the density of a $\mathcal{N}(1_{\{k_0=1\}}, 1)$ (red curve). The Kolmogorov–Smirnov tests are now conducted for this distribution. For $k_0 = 1$, where asymptotic power is present, convergence toward the limit distribution is slower than in the null hypothesis, particularly in terms of the variance.

Third, we considered finite Sobolev tests with $k_0 > 1$ positive weights for the same integrated von Mises–Fisher alternatives. According to the comments after Theorem 2.2:

i. $\Gamma = 0$ for the sequence of weights $v_{k,d_n} = 1_{\{k \leq k_0\}}$.

ii. $\Gamma = 1/\sqrt{2}$ for the sequence of weights $v_{k,d_n} = \delta_{k,1} + [k!d_n^{-k}]^{1/4}1_{\{1 < k \leq k_0\}}$.

Considering $\tau^2 = \sqrt{2}$, then $\sigma_n^{-1}T_n \rightsquigarrow \mathcal{N}(0, 1)$ for the first case and $\sigma_n^{-1}T_n \rightsquigarrow \mathcal{N}(1, 1)$ for the second. Figures 4 and 5 illustrate these behaviors when $k_0 = 3$ (i.e., only the first weights are positive).

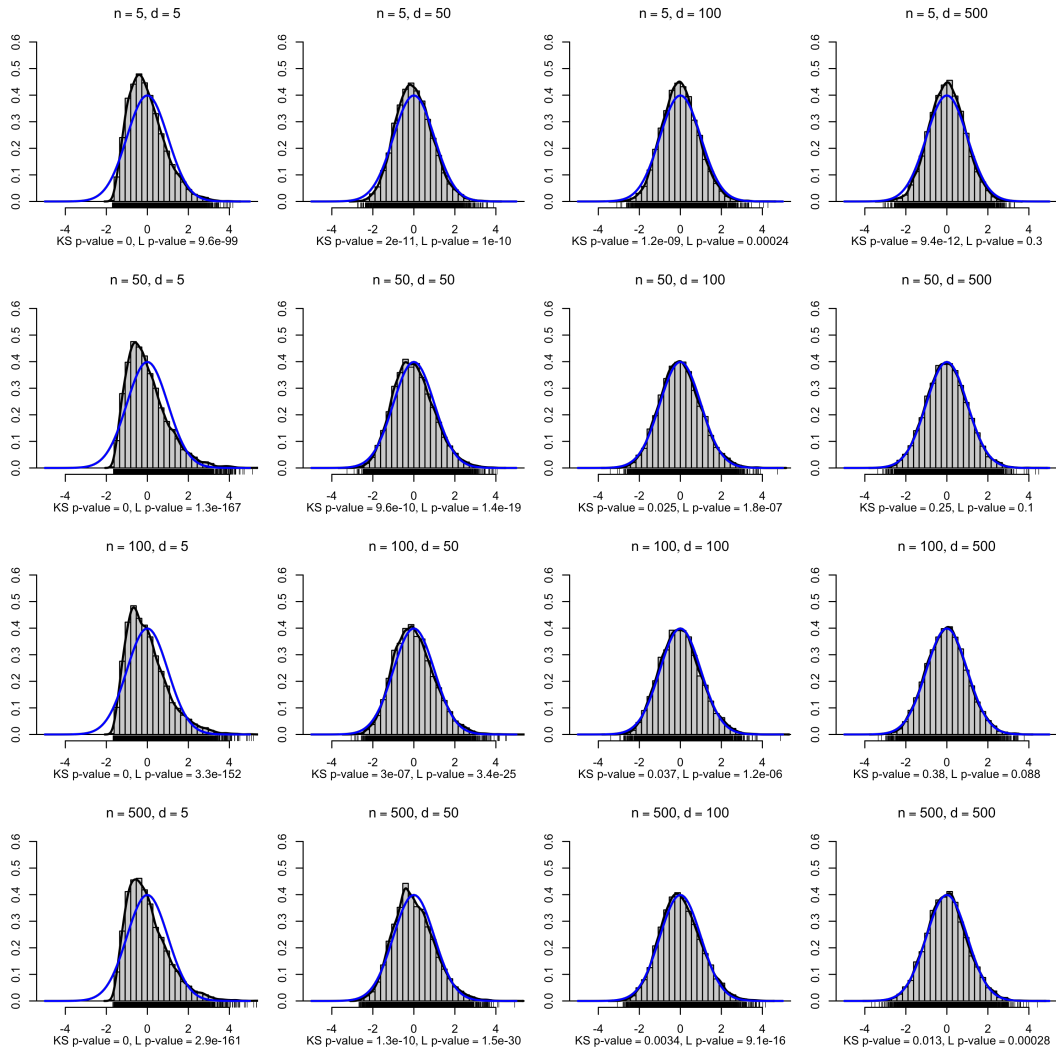


Figure 1: Empirical evaluation of $\tilde{T}_{n,k_0} \rightsquigarrow \mathcal{N}(0, 1)$ under $\mathcal{H}_{0,n}$ for $k_0 = 1$.

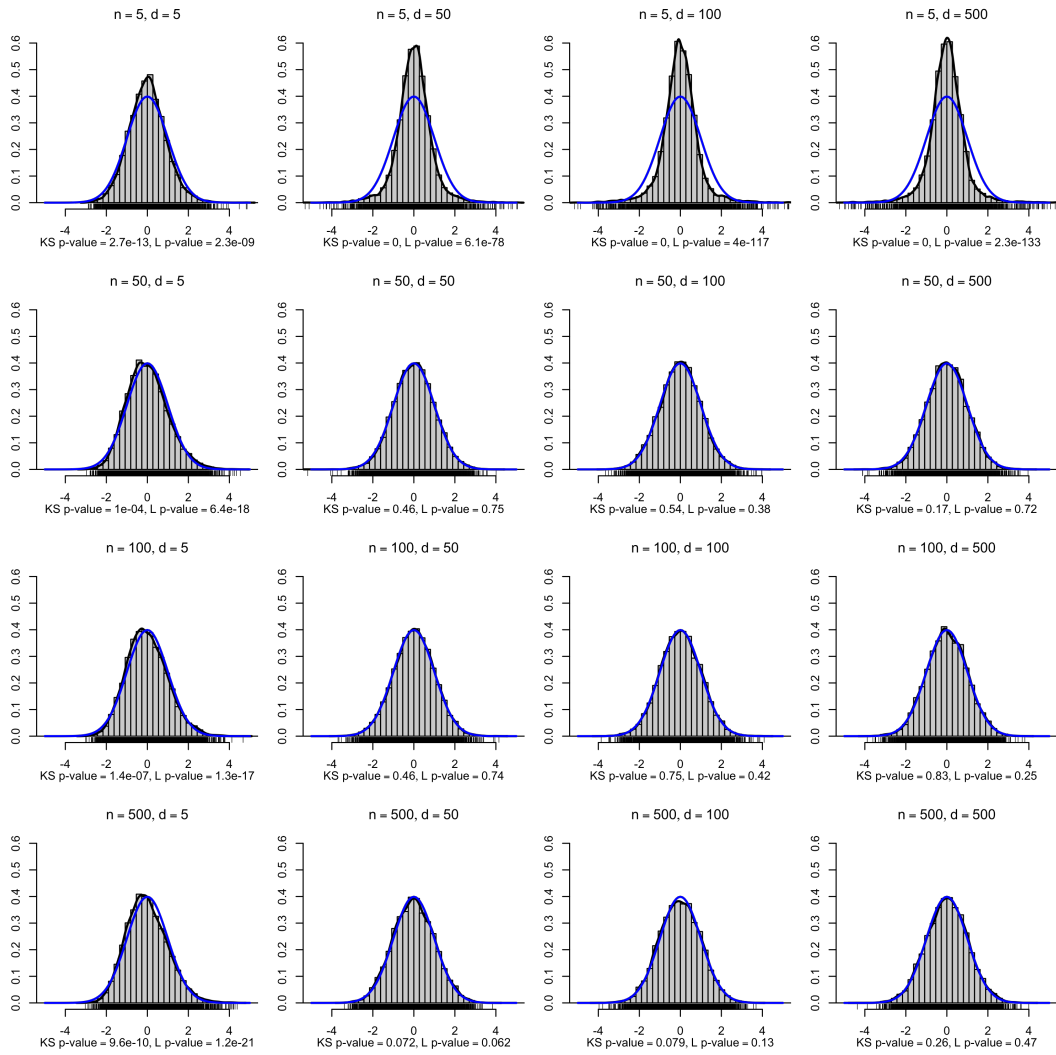


Figure 2: Empirical evaluation of $\tilde{T}_{n,k_0} \rightsquigarrow \mathcal{N}(0, 1)$ under $\mathcal{H}_{0,n}$ for $k_0 = 3$.

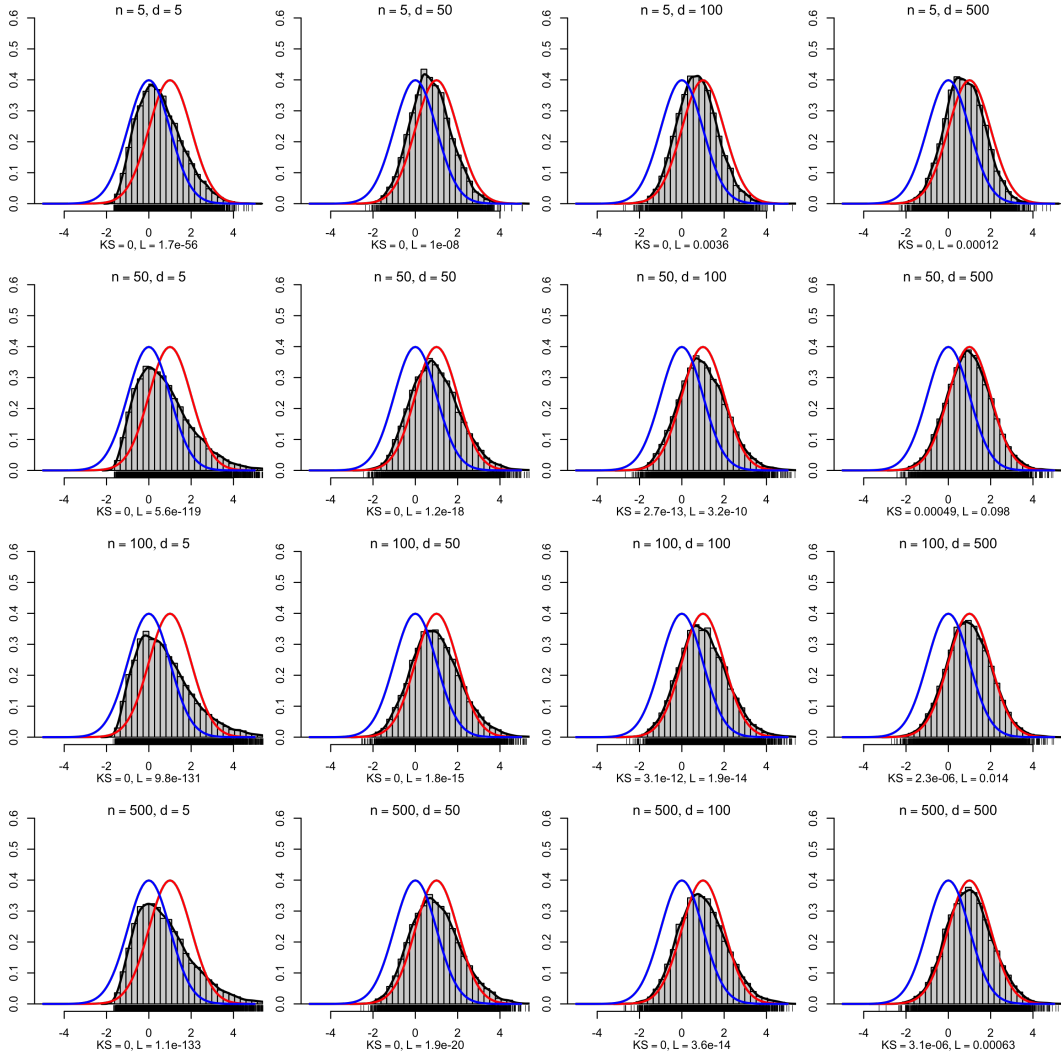


Figure 3: Empirical evaluation of $\tilde{T}_{n,k_0} \rightsquigarrow \mathcal{N}(1, 1)$ under $\mathcal{H}_{1,n}$ for $k_0 = 1$.

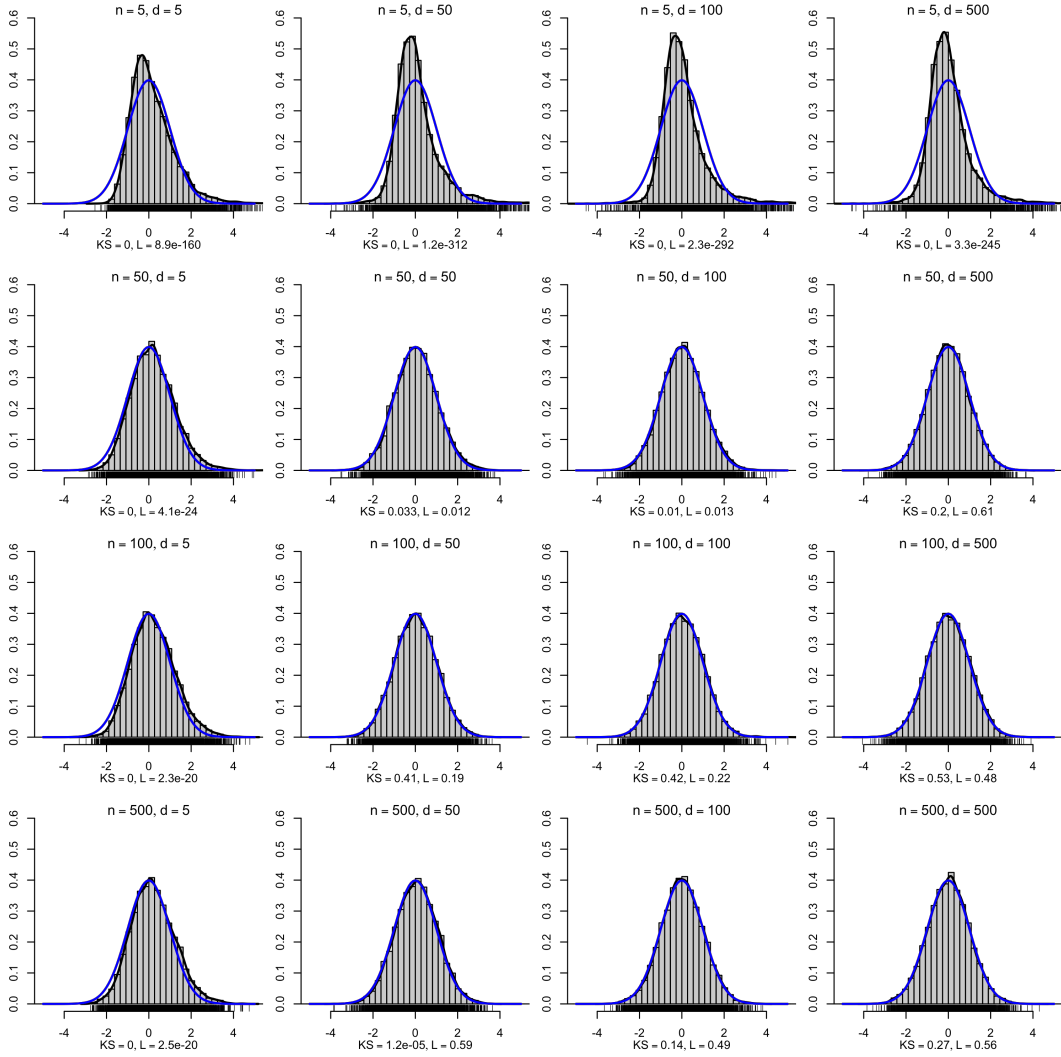


Figure 4: Empirical evaluation of $\sigma_n^{-1} T_n \rightsquigarrow \mathcal{N}(0, 1)$ under $\mathcal{H}_{1,n}$ with $v_{k,d_n} = 1_{\{k \leq k_0\}}$ and $k_0 = 3$.

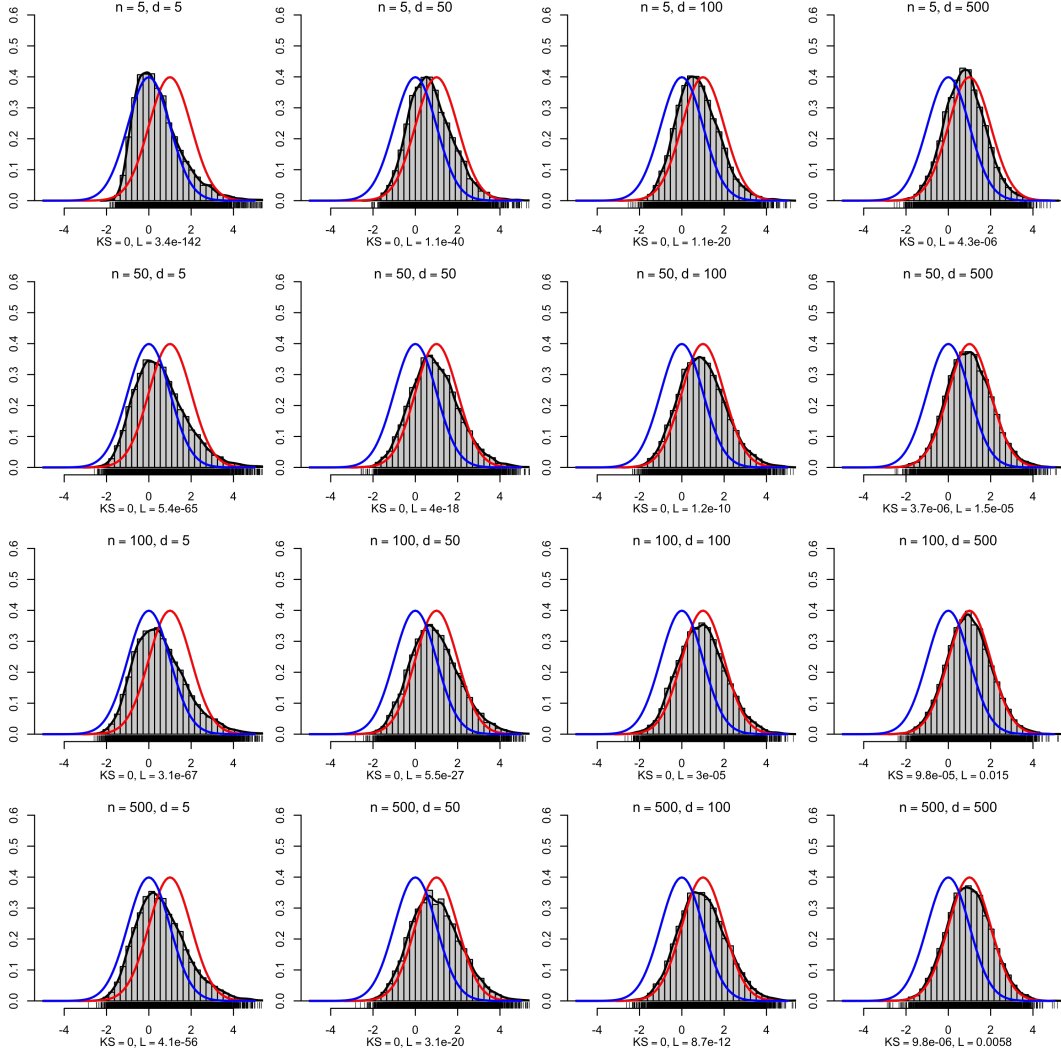


Figure 5: Empirical evaluation of $\sigma_n^{-1}T_n \rightsquigarrow \mathcal{N}(1, 1)$ under $\mathcal{H}_{1,n}$ with $v_{k,d_n} = \delta_{k,1} + [k!d_n^{-k}]^{1/4}1_{\{1 < k \leq k_0\}}$ and $k_0 = 3$.